Elastic scattering of hadrons at high energies

L. S. Zolin, A. B. Kaĭdalov, V. A. Sviridov, L. N. Strunov, and I. V. Chuvilo

Joint Institute for Nuclear Research; Institute of Theoretical and Experimental Physics
Usp. Fiz. Nauk **117**, 119–158 (September 1975)

This review is concerned with the experimental data on elastic scattering of mesons and nucleons by protons. Theoretical ideas about hadronic interactions at high energies are discussed. An exposition is given of the techniques for measuring differential cross sections in the region of very small momentum transfers. A summary is given of the information which has been obtained in various experiments on the total cross sections for $\pi^{\pm}N$, $K^{\pm}N$, NN, and $\bar{N}N$ interactions, the real parts of the elastic scattering amplitudes at $t=0$, the slopes of the diffraction peaks, large-angle scattering, and polarization effects in elastic scattering reactions. It is observed that the entire set of experimental data is consistent with dispersion relations and asymptotic theorems. The slope of the diffraction peak exhibits a systematic (approximately logarithmic) growth at high energies. This growth corresponds to a relatively small value for the slope of the Pomeranchuk trajectory, $\alpha_P'(0) \approx 0.3$ GeV^{-2}. The experimental data in elastic scattering processes and charge-exchange reactions are in agreement with the predictions of complex angular momentum theory. A discussion is given of new phenomena which have been observed using the accelerators at Serpukhov and Batavia and the CERN intersecting storage rings: a growth of the total cross sections for hadronic interactions, a change of sign of the real part of the zero-angle elastic scattering amplitude, and other effects which show up at energies $\gtrsim 100$ GeV.

PACS numbers: 13.80.D

CONTENTS

1. INTRODUCTION

1.1. Subject of the Review

This review is concerned with the experimental data on elastic scattering of mesons and nucleons by protons. Investigations which have been carried out in the past decade, both in the U.S.S.R. and on foreign accelerators, have led to major modifications in the picture of the interactions of hadrons and their structure which was built up in the early 1960s: the observation of a significant interference between the Coulomb and nuclear scattering in experiments on the scattering of protons and pions showed the limitations of a purely diffractive treatment of the scattering of hadrons at high energies (E ~ 1–10 GeV). It is now clear that, even at energies hundreds of times higher (E ~ 100–1000 GeV), the nature of the interaction is nothing like the asymptotic behavior which was predicted in the early 1960s: with increasing energy, the total cross sections have begun to rise, the real part of the pp scattering amplitude continues to rise instead of tending rapidly to zero as previously expected, and there is also a growth in the radius of interaction.

We shall describe here the information which has been obtained in recent years from experimental studies of total cross sections, interference between Coulomb and nuclear scattering, and polarization. A common feature of all these experiments is that they involve, on the whole, the study of properties of the amplitude for elastic scattering of the particles. For example, owing to the unitarity condition, which leads to the optical theorem, measurements of the total cross sections σ_t make it possible to calculate the imaginary part of the elastic scattering amplitude in the forward direction. By analyzing differential cross sections for elastic scattering in the small-angle region, where the Coulomb interaction is important, the magnitude of the interference effect can be used to determine the real part of the nuclear amplitude at scattering angles near zero.

The characteristic features of elastic scattering of high-energy hadrons can be seen from Fig. 1, in which we show differential cross sections for the elastic scattering of hadrons by protons at a momentum p = 5 GeV/c. A common feature of all the processes is the presence of maxima for forward and backward scattering, which are apparently related to the exchange character of the scattering. The forward peak is due to the t-channel singularities, and the backward peak is due to the u-channel singularities. The peaks are separated by a large region in which the cross sections are 5–6 orders of magnitude lower than the "optical points" for the corresponding processes. All reactions except those having no direct-channel resonances are characterized by the presence of structures in the differential cross section $d\sigma/dt$ in the range $0.5 \lesssim -t \lesssim 3$ (GeV/c)^2. This range of momentum transfers is a region of transition from a regime of scattering by the nucleon as a whole to one of scattering with large momentum transfers, which may be associated with scattering by the substructure of the nucleon.

As can be seen from Fig. 1, the t-dependence of $d\sigma/dt$ in this transition region is generally not monotonic and may be a result of interference effects. The structure in the t-dependence of $d\sigma/dt$ is correlated with the features of the t-dependence of the polarization. With the advent of experiments in the region of large scattering angles, where the energy and angular dependences of the differential cross sections have a completely different form than in the diffraction cone, it has become possible to decide whether the nucleon is elementary

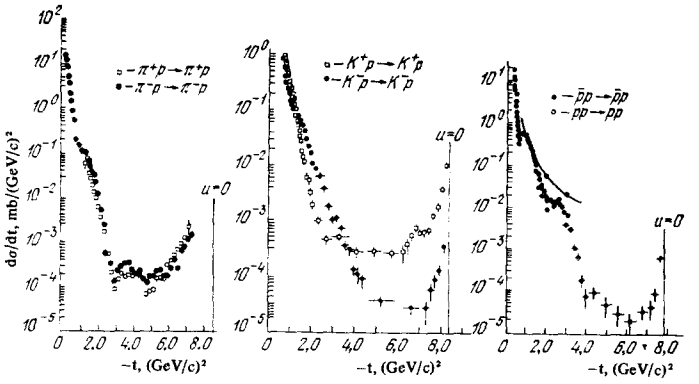

FIG. 1. Differential cross sections for the elastic scattering of hadrons by protons at 5 GeV/c [38].

and, if not, to study its internal structure. As in Rutherford's time, experiments on elastic scattering continue to play the leading role in elucidating the nature of the strong interactions.

1.2. The Scattering Amplitude

The process of elastic scattering of spinless particles 1 and 2

$$1 + 2 \to 1' + 2' \tag{1.1}$$

is described by a scattering amplitude T(s, t), which is a function of the kinematic invariants s, t and u, the latter being related to the 4-momenta of the particles before the scattering, p_i, and after the scattering, p_i', by the equations

$$\left.\begin{aligned} s &= (p_1 + p_2)^2 = (p_1' + p_2')^2, \\ t &= (p_1' - p_1)^2, \\ u &= (p_1 - p_2')^2. \end{aligned}\right\} \tag{1.2}$$

If the particles which participate in a reaction have spins, the scattering amplitude depends not only on the kinematic invariants s, t and u, but also on invariants constructed from the wave functions of the particles, the number of which is restricted by the condition that the strong interactions are symmetric with respect to P, C and T transformations. In particular, in the case of scattering of a pion (spin 0) by a proton (spin 1/2), the process is described by two independent amplitudes; for scattering of spin-1/2 particles by spin-1/2 particles (pp → pp, for example), the amplitude consists of five terms. In the first case, the nuclear amplitude for elastic scattering in the small-angle region contains a total of two real parameters, T = Re T + i Im T, and their ratio ρ = Re T/Im T can be determined by measuring the interference between the Coulomb and nuclear scattering. In the case of pp scattering, when both particles have spin, analyses of experimental data at $t \sim 0$ are generally carried out under the assumption that the proton-proton interaction in the high-energy region is the same in the triplet and singlet states.

The differential cross section is related to the Coulomb amplitude T_C and the nuclear scattering amplitude by the formula

$$\frac{d\sigma}{dt} = \frac{|T_C(1 + 2i\eta) + T|^2}{64\pi p^2 s}; \tag{1.3}$$

here η is the phase shift between the Coulomb and nuclear scattering ($\eta \sim 10^{-2}$ in the Coulomb-nuclear interference region). The t-dependence of the nuclear amplitude is usually approximated by an exponential exp (Bt) and, using the optical theorem,

$$\operatorname{Im} T(t) = 2p\sqrt{s}\,\sigma_t \exp\left(\frac{Bt}{2}\right). \tag{1.4}$$

Since the Coulomb amplitude T_C is known from theory, while the imaginary part of the nuclear amplitude T for $t \sim 0$ is determined by the value of the total cross section according to the optical theorem, the results of measurements can be used to extract the interference contribution $\sim 2T_C \operatorname{Re} T$ and hence determine Re T.

To determine the slope parameter B, measurements are made in a larger interval $10^{-3} \leq -t \leq 10^{-1}$ (GeV/c)^2. In determinations of the parameter ρ and B by means of interference experiments, the value of Im T (t = 0) is usually calculated from data on the total cross sections, which are measured with a high degree of accuracy by the transmission method. In colliding-beam experiments, where the transmission method is inapplicable, the total interaction cross section can be determined from the differential cross sections for elastic scattering, including the interference region, by applying the optical theorem

$$\sigma_t = \frac{\operatorname{Im} T(t=0)}{2p\sqrt{s}}. \tag{1.5}$$

We note that, before the advent of interference experiments, attempts were made to estimate the real part of the elastic scattering amplitude from the amount by which the extrapolation of the differential cross section to zero angle exceeds the "optical" limit $\sim |\operatorname{Im} T(0)|^2$. Apart from the fact that the sign of Re T is not determined by this method, this procedure of extracting information about Re T is itself very unreliable: firstly, the excess may be due not only to Re T, but also to spin effects; secondly, this procedure is very sensitive to the ambiguities in the absolute normalization of the cross sections and, finally, to the choice of the empirical formula for extrapolating the cross sections to zero angle. This last circumstance was of particular importance for the early estimates, since the methods that were then available for carrying out the measurements did not work in the region of momentum transfers sufficiently close to zero.

Thus, in the region $t \sim 0$, the amplitude for elastic scattering of pions (and, in a certain approximation, protons) by protons is completely determined by measurements of the total interaction cross sections of these particles and the differential cross sections for elastic scattering in the Coulomb-nuclear interference region.

The scattering of a spinless particle by a nucleon at an arbitrary angle is described in the general case by two complex amplitudes $f_{++}(s, t)$ and $f_{+-}(s, t)$, where "+" and "−" are the signs of the helicities of the initial and final nucleons. At zero scattering angle ($t \sim 0$),

only the single amplitude f_{++} remains, corresponding to conservation of the helicity of the nucleon. By virtue of isotopic invariance, the amplitudes for the processes

$$\pi^{\pm}p \to \pi^{\pm}p, \tag{1.6}$$

$$\pi^{-}p \to \pi^{0}n \tag{1.7}$$

can be expressed in terms of the two independent isotopic amplitudes f^0 and f^1:

$$\begin{aligned} f(\pi^{\pm}p \to \pi^{\pm}p) &= f^0 \pm f^1, \\ f(\pi^{-}p \to \pi^{0}n) &= \sqrt{2}\, f^1. \end{aligned} \tag{1.8}$$

The amplitudes f^0 and f^1 correspond to isotopic spin 0 and 1 in the t-channel.

Thus, there are eight real functions which completely determine the πN scattering amplitudes. These quantities can be determined from experimental data on the differential cross sections, polarizations, and spin rotation parameters R and A, which can be expressed as follows in terms of the amplitudes f_{++} and f_{+-}:

$$\frac{d\sigma}{dt} = \frac{\pi(|f_{++}|^2 + |f_{+-}|^2)}{p^2}, \tag{1.9}$$

$$P = -\frac{2\,\mathrm{Im}\,(f_{++} f_{+-}^{*})}{|f_{++}|^2 + |f_{+-}|^2}, \tag{1.10}$$

$$R(|f_{++}|^2 + |f_{+-}|^2) = -(|f_{++}|^2 - |f_{+-}|^2)\cos\theta_L - 2\,\mathrm{Re}\,(f_{++} \cdot f_{+-}^{*})\sin\theta_L, \tag{1.11}$$

$$A(|f_{++}|^2 + |f_{+-}|^2) = (|f_{++}|^2 - |f_{+-}|^2)\sin\theta_L - 2\,\mathrm{Re}\,(f_{++} \cdot f_{+-}^{*})\cos\theta_L, \tag{1.12}$$

where θ_L is the scattering angle of the recoil nucleon in the laboratory system. It is obvious that measurements of these quantities in the processes (1.6) and (1.7) are sufficient for the reconstruction of all the amplitudes, apart from the ambiguity of a common phase.

As we have already mentioned, the common phase of the amplitudes at t = 0 can be determined from the data on $\sigma_t^{\pi N}$ and the Coulomb interference by using the optical theorem. At non-zero angles, the common phase cannot be determined directly from the experimental data on πN scattering, but can be found by indirect methods.

The amplitude analysis of pp scattering is much more complicated: experiments are required not only with a polarized target, but also with a polarized beam.

2. GOALS AND METHODS OF STUDYING THE ELASTIC SCATTERING OF HADRONS

Experimental data on the elastic scattering of hadrons play a major role in our understanding of the entire picture of strong interactions at high energies: they provide a means of testing the consequences of the fundamental principles of the theory (we have in mind tests of dispersion relations, sum rules and asymptotic relations). These same data also constitute a basis for constructing particular theoretical models describing the strong-interaction mechanism: models involving the exchange of reggeized particles, optical and quasi-potential models, the quark model, and many others.

2.1. Theoretical Aspects of the Problem of Hadronic Scattering at High Energies

Principles such as Lorentz invariance, unitarity, analyticity and crossing play a fundamental role in the relativistic quantum theory. By virtue of Lorentz invariance, the scattering amplitude f(ab → a'b') for spinless particles is a scalar function of the two independent invariants s and t.

A major dynamical principle of the theory is the unitarity condition for the S-matrix,

$$S^{+}S = 1, \tag{2.1}$$

which is a consequence of the superposition principle and the conservation of the normalization of states in quantum mechanics. The unitarity condition leads, in particular, to the optical theorem

$$\mathrm{Im}\, f(s, 0) = \frac{p\sigma_t}{4\pi}. \tag{2.2}$$

If the amplitude for elastic scattering is expanded in partial waves,

$$f(s, t) = \frac{1}{p}\sum_{l=0}^{\infty}(2l+1)\,P_l(\cos\theta_s)\,f_l(s), \tag{2.3}$$

the unitarity condition implies a bound on the magnitudes of the partial-wave amplitudes:

$$\mathrm{Im}\, f_l(s) \geqslant |f_l(s)|^2, \quad |f_l(s)| \leqslant 1. \tag{2.4}$$

The equality is attained for energies below the threshold for inelastic processes, when only elastic scattering is possible. The property (2.4) of the partial-wave amplitudes is used in proving a number of asymptotic theorems.

Analyticity is an important property of scattering amplitudes. In a number of cases, the analytic properties of the amplitude can be rigorously proved in the framework of quantum field theory[1] and are in fact a consequence of the principle of microcausality.

In the relativistic quantum theory, a single analytic function T(s, t, u) describes each of the processes a + b → a' + b' (the so-called s-channel of the reaction), a + $\bar{a}'$ → $\bar{b}$ + b' (the t-channel) and a + $\bar{b}'$ → a' + $\bar{b}$ (the u-channel), although the ranges of variation of the invariant variables for these processes are different. This property, which provides an interrelationship between the amplitudes for different physical processes, is often called crossing. If b = $\bar{b}'$ (b = $\bar{a}'$), the amplitude must be symmetric with respect to the interchange s ⇄ u (s ⇄ t) (crossing symmetry).

a) **Dispersion relations and theoretical asymptotic predictions.** Using the analytic properties of the amplitude T(s, t) and crossing, it is possible to derive the so-called dispersion relation[1)]

$$= \frac{c_1}{s_1 - s} + \frac{c_2}{u_1 - u} + \frac{\mathcal{P}}{\pi}\int_{s_2}^{\infty}\frac{\mathrm{Im}\,T(s' + i\varepsilon, t)}{s' - s}\,ds' + \frac{\mathcal{P}}{\pi}\int_{u_2}^{\infty}\frac{\mathrm{Im}\,T(u' + i\varepsilon, t)}{u' - u}\,du. \tag{2.5}$$

The symbol $\mathcal{P}$ indicates that the principal value of the integral is taken, s_1 and u_1 correspond to the squares of the masses of the stable particles in the s- and u-channels, and s_2 and u_2 correspond to the thresholds for two-particle production in the corresponding channels. Let us consider the dispersion relations for πN forward elastic scattering (t = 0) in greater detail. Taking into account the crossing symmetry of the scattering amplitudes, it is convenient to consider the particular combinations of amplitudes

$$\begin{aligned} T^{+}(E) &= \tfrac{1}{2}[T_{+}(E) + T_{-}(E)], \\ T^{-}(E) &= \tfrac{1}{2}[T_{-}(E) - T_{+}(E)], \end{aligned} \tag{2.6}$$

where $T_+(E)$ and $T_-(E)$ are the amplitudes for elastic π^+p and π^-p scattering, respectively, and E = (s − t − u)/

[1)] This relation is valid if T(s, t) → 0 as s → ∞. If this condition is not satisfied, a subtracted dispersion relation must be written.

4m is the energy in the laboratory system. Using the general properties of analyticity and unitarity, we can write a once-subtracted dispersion relation for the symmetric amplitude. When comparisons are made with experimental data, the dispersion relations are most frequently used in the form[3,4]

$$D^+(E) = D^+(\mu) + \frac{f^2k^2[E^2-(\mu^2/2m)^2]^{-1}}{m[1-(\mu/2m)^2]} + \frac{k^3}{4\pi^2}\mathcal{P}\int_\mu^\infty \frac{dE'}{k'}\frac{k'(\sigma_- + \sigma_+)}{(E'^2-E^2)}, \quad (2.7)$$

$$D^-(E) = 2f^2E\left[E^2-\left(\frac{\mu^2}{2m}\right)^2\right]^{-1} + \frac{E}{4\pi^2}\mathcal{P}\int_\mu^\infty dE'\frac{k'(\sigma_- - \sigma_+)}{E'^2-E^2}, \quad (2.8)$$

where $D^\pm(E) = \mathrm{Re}\, T^\pm(E)\, k/8\pi p\sqrt{s}$, $f^2 = 0.80 \pm 0.03$ is the pion-nucleon coupling constant, $k = \sqrt{E^2-\mu^2}$ is the momentum in the laboratory system, and μ and m are the masses of the pion and nucleon.[2)]

The dispersion relation for $D^-(E)$ in the form (2.8) is written without subtractions, with the assumption that the differenee of cross sections $\sigma_- - \sigma_+$ falls off as $E \to \infty$ in such a way that $\lim (\sigma_- - \sigma_+) \ln E \to 0$. The basis for this assumption is the Pomeranchuk relation.[5] An analysis of the integrands in Eqs. (2.7) and (2.8) indicates that the values of $D^\pm(E)$ at small E depend little on the asymptotic total cross sections.[4]

With a measurement of the real part of the elastic forward scattering amplitude at an energy E_1, together with the results of measurements of the total cross sections σ_t within a wide interval of E, it is possible to carry out quantitative tests of the dispersion relations and hence of the basic principles of local field theory.

The complex picture of the strong interactions must evidently become simpler at very high energies, when $s \to \infty$, and the scattering amplitudes then satisfy a number of asymptotic relations. One of the first such relations, establishing the equality of the total cross sections for particle and antiparticle interactions as $s \to \infty$, was derived in 1958 by Pomeranchuk,[5] whose proof made use of dispersion relations and the assumption that the effective radius of interaction remains finite as $s \to \infty$. Somewhat later, Pomeranchuk's result was derived on more general grounds.[6] The assumption that the asymptctic radius of interaction is finite may be replaced by the weaker hypothesis that

$$\lim_{s\to\infty} \frac{\mathrm{Re}\, T(s, t=0)}{\mathrm{Im}\, T(s, t=0)} \frac{1}{\ln(s/s_0)} \to 0. \quad (2.9)$$

Pomeranchuk's relation can be generalized to the differential cross sections for the elastic scattering of particles and antiparticles:[7]

$$\lim_{s\to\infty}\left[\frac{d\sigma}{dt}(a+b\to a+b)\Big/\frac{d\sigma}{dt}(\bar a+b\to\bar a+b)\right] = 1. \quad (2.10)$$

Another important constraint on the scattering amplitude as $s \to \infty$ was obtained by Froissart.[2] By using the analytic properties of the elastic scattering amplitude in the variable t, i.e., taking into account the fact that the nearest singularity in t (at $t = 4\mu^2$) lies at a finite distance from the physical region of the s-channel ($t < 0$), it can be shown that the highest partial waves in (2.3) which can contribute significantly to the scattering amplitude as $s \to \infty$ are subject to the condition

$$l_{\max} = L \leqslant c\frac{\sqrt{s}}{\mu}\ln s, \quad (2.11)$$

where c is some constant, and μ is the mass.

Equation (2.11) and the constraint (2.4) on the partial-wave amplitudes lead to the Froissart bound[2] on the rate of growth of the amplitude as $s \to \infty$:

$$|T(s, 0)| \leqslant \mathrm{const}\cdot s\ln^2 s; \quad \sigma_t(s) \leqslant \mathrm{const}\cdot\ln^2 s. \quad (2.12)$$

The inequality (2.11) also leads to an important bound on the value of the slope of the diffraction peak, $B(s) = d \ln (d\sigma/dt)_{t=0}/dt$:

$$B(s) \leqslant \mathrm{const}\cdot\ln^2 s \ \text{ as } \ s\to\infty. \quad (2.13)$$

The asymptotic inequalities have been widely studied in recent years; in particular, the constants in the inequalities (2.11)–(2.13) have been fixed. Inequalities which should be satisfied even at non-asymptotic energies have also been obtained.[8] Discussions of the recent results obtained in this area can be found in the reviews [7,9].

b) **Theoretical models.** 1) **Optical models.** At high energies, the large values $l \sim pR$, where R is the radius of interaction, play a major role in the partial-wave expansion (2.3) of the scattering amplitude. Therefore, using the fact that $P_l(\cos\theta) \approx J_0((l+1/2)\theta)$, where J_0 is the Bessel function of order zero, we can write the small-angle scattering amplitude in the form

$$T(s, t) = 8\pi\sqrt{s}f(s,t) \approx 16\pi\int_0^\infty f_l(s)J_0(l\theta)\,dl^2 \approx 4\pi s\int_0^\infty f(s, b)J_0(qb)\,db^2, \quad (2.14)$$

where $b = l/p$ is the impact parameter, and $q = p\theta \approx \sqrt{-t}$. Using the fact that the momentum transfer vector q is transverse for $\theta \ll 1$ and introducing a transverse vector b in impact-parameter space, the relation (2.14) can also be written in the form

$$T(s, t) = 4s\int_0^\infty f(s, b)e^{iqb}\,d^2\mathbf{b}. \quad (2.15)$$

The amplitude f(s, b) satisfies the bounds (2.4) and can be represented in the form

$$f(s, b) = \frac{1}{2i}(e^{2i\delta(s, b)} - 1), \quad (2.16)$$

with $\mathrm{Im}\,\delta(s, b) \geq 0$ (the equality sign holds when there is only elastic scattering).

The representation of the amplitude in the form (2.14)–(2.16) is often used for the construction of optical or geometric models. Let us consider the simplest example. Suppose that, owing to the presence of a large number of open channels at high energy, the incident wave experiences strong absorption for impact parameters $b \leq R$; then $\mathrm{Im}\,\delta(s, b) \gg 1$ for $b \leq R$, i.e., $f(s, b) = i/2$ in this region but is otherwise equal to zero. This model corresponds completely to diffraction by a black sphere of radius R.

In this case, it follows from Eq. (2.14) that

$$T(s, t) = isF(t), \quad \sigma_t = 2\sigma_e = 2\pi R^2, \quad (2.17)$$

where

$$F(t) = 4\pi R^2\cdot J_1(qR)/qR.$$

The differential cross section for elastic scattering is maximal at $t = 0$ and falls off by a factor e when t varies by an amount $\sim 1/R^2$, i.e., the width of the diffraction peak is inversely proportional to R^2 (this is also true for a more realistic form of the function f(s, b)). As we have already mentioned, it follows from the general

[2)] Henceforth we employ units such that $h = c = 1$.

principles of S-matrix theory that

$$R \sim b_{\max} = \frac{L}{p} \leqslant \text{const} \cdot \frac{\ln s}{\mu}.$$

The foregoing model of scattering by a black sphere with a sharp edge is highly simplified and provides only a qualitative picture of the character of elastic scattering in the small-angle region. Analyses of experimental data make use of more realistic models,[10] which take into account transparency, the real part of the amplitude, the diffuseness of the edge, etc.

2) The Regge pole model. In the framework of complex angular momentum theory, the scattering amplitude at high energies is determined by the singularities of the partial-wave amplitudes in the crossed t-channel, $\varphi(j, t)$, which are functions of the complex orbital angular momentum $j(t)$.[3] Essential use is made here of the properties of analyticity and crossing of the scattering amplitudes. The unitarity condition in the t-channel is usually used to obtain information about the singularities of $\varphi(j, t)$. It follows from the two-particle unitarity condition in the t-channel that, as in the nonrelativistic theory, $\varphi(j, t)$ has poles at the points $j = \alpha_i(t)$—the Regge poles. The scattering amplitude in the Regge-pole model has the simple form

$$T(s, t) = \sum_i b_i^{\sigma}(t)\, \eta(\alpha_i^{\sigma}(t)) \left(\frac{s}{s_0}\right)^{\alpha_i(t)}, \qquad (2.18)$$

where $\eta(\alpha_i^{\sigma}(t)) = -(1 + \sigma \exp(-i\pi\alpha_i(t))/\sin \pi\alpha_i(t))$ is the signature factor, and $\sigma = \pm 1$ is the signature; $b_i(t)$ is the residue, which is a real function of t in the s-channel physical region and which also satisfies the factorization condition $b_i(t) = g_i^{bb'}(t) g_i^{aa'}(t)$, where $g_i^{aa'}(t)$ is a vertex depending only on the properties of aa'. The explicit form of the functions $g(t)$ is not predicted by the theory. The exchange of a Regge pole can be represented by the graph shown in Fig. 2.

A Regge pole generalizes the concept of the exchange of an elementary particle with a definite value of the spin to the case of arbitrary values lying on a trajectory $j(t)$. Like an ordinary particle, a Regge pole has definite values of the conserved quantum numbers, such as parity, isospin and strangeness. The relation between Regge poles and resonant states makes it possible to make use of information on the spectrum of particles and resonances to determine the parameters of the trajectories and thus to predict the energy dependence of scattering processes. The main boson Regge poles which exist are as follows: first of all, there is the Pomeranchuk (or vacuum) pole P with $\alpha_P(0) = 1$, which is responsible for the constancy of the total cross sections at high energies; this pole has $\sigma = +1$ and hence automatically guarantees that the Pomeranchuk relation is satisfied; in addition, there are the secondary poles f, A_2, ω and ρ with $\alpha_i(0) \sim 0.5$, which contain the corresponding resonances. It follows from the spectrum of particles and resonances that all the secondary poles have $\alpha_i' \equiv (d\alpha/dt)|_{t=0} \approx 1$ GeV^{-2}.

If, at very high energies, allowance is made for only the Regge pole which lies furthest to the right, with the largest value of $\alpha(0)$, then the differential cross section has the form

$$\frac{d\sigma}{dt} = \frac{b^2(t)}{16\pi} |\eta(\alpha(t))|^2 \left(\frac{s}{s_0}\right)^{2(\alpha(t)-1)}. \qquad (2.19)$$

[3] A detailed exposition of Regge-pole theory and a comparison of its predictions with experimental data can be found, for example, in the reviews [11-13].

FIG. 2. The graph representing the exchange of a Regge pole.

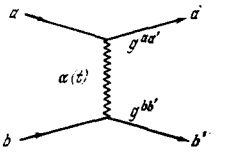

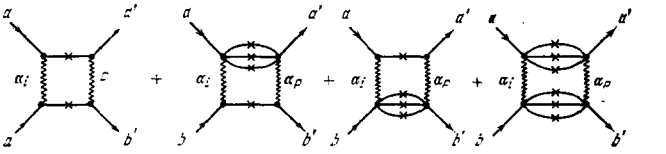

FIG. 3. Graphs corresponding to the exchange of branch points in the t-channel. The crosses on the lines indicate that the particles are taken on the mass shell.

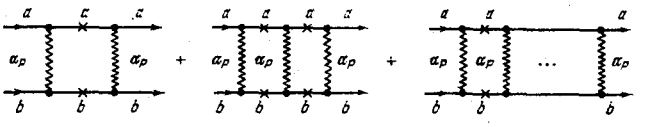

FIG. 4. Graphs corresponding to elastic rescattering by the P Regge pole.

By expanding $\alpha(t)$ in a series in t, we find that at small t

$$\frac{d\sigma}{dt} \sim \left(\frac{s}{s_0}\right)^{2(\alpha(0)-1)} \exp\left[2\alpha' t \ln\left(\frac{s}{s_0}\right)\right] F_1(t). \qquad (2.20)$$

At very high energies, when $2\alpha' \ln(s/s_0) \gg 1/m^2$, it follows from Eq. (2.20) that the slope of the diffraction peak rises like $\sim \ln(s/s_0)$ (the width of the peak accordingly shrinks like $\sim 1/\ln(s/s_0)$). This means that the effective radius of interaction grows like $\sim \sqrt{\ln(s/s_0)}$ in the Regge-pole model. The constancy of the total interaction cross section (for $\alpha_P(0) = 1$) is a result of the fact that the partial-wave amplitudes $f(s, b)$ fall off logarithmically as $s \to \infty$. This means that, in addition to the growth of the effective radius of interaction, a hadron becomes more and more transparent with increasing energy.

Unfortunately, Regge poles are not the only singularities in the j-plane. In a relativistic theory, there are also multi-particle terms in the t-channel unitarity condition, and a theoretical analysis[14] shows that they lead to the appearance of new singularities—moving branch points—in the j-plane. These branch points correspond to the exchange of several Regge poles in the t-channel. The asymptotic picture of scattering becomes more complicated when allowance is made for the branch points, although many predictions of the Regge-pole model remain valid (see, e.g., the lecture[15]). The branch points may be regarded as representing the successive rescatterings corresponding to the graphs shown in Fig. 3 (as an example, we show a two-reggeon branch point).

If a summation is made of all the vacuum branch points which correspond to purely elastic rescatterings, i.e., the graphs of Fig. 4, then the scattering amplitude can be written[4] in a compact form corresponding to the eikonal representation (2.15) and (2.16), where

$$\delta(s, b) = \delta_P(s, b) = \frac{1}{8\pi s} \int T_P(s, t)\, e^{-iqb} \frac{d^2q}{2\pi}. \qquad (2.21)$$

Here $T_P(s, t)$ is the amplitude (2.18) corresponding to exchange of the P Regge pole.

The most complete quantitative description of exper-

imental data on elastic scattering and charge-exchange processes within the framework of the Regge-pole model with allowance for branch points has been given in [17]. Moving branch points due to successive rescatterings by the constituent particles of a hadron lead to the appearance of characteristic minima in the differential cross sections for elastic scattering and charge-exchange processes, these being analogous to effects which occur in describing the scattering of particles by nuclei by means of the Glauber approach.[18] The analogy with scattering by nuclei also makes it possible to understand a number of other qualitative effects due to branch points. Branch points in the amplitude for elastic scattering correspond to screening and have a sign opposite to that of a Regge-pole contribution. With increasing energy, a hadron becomes "more and more" transparent, and the screening decreases. This leads to a pre-asymptotic growth of the total cross sections.[19] The ratio $\mathrm{Re}\,T(s,0)/\mathrm{Im}\,T(s,0)$ must become positive at very high energies and must fall off like $\sim 1/\ln^2 s$ as $s \to \infty$.

3) The quasi-potential. As we have pointed out, the amplitude at high energies and small scattering angles can be represented in the eikonal form (2.14)–(2.16). In nonrelativistic quantum mechanics, the phase $\delta(s,b)$ can be expressed in terms of the potential V as follows:

$$\delta(b)=\frac{1}{2p}\int_{-\infty}^{\infty} V\left(\sqrt{b^2+z^2}\right)dz, \tag{2.22}$$

where z is the coordinate in the direction of motion of the particle.

In a relativistic quantum theory, we can introduce a quantity $V(s,r)$—the quasi-potential,[20] which is a generalization of the ordinary potential. In the quasi-potential method,[21,22] the amplitude for elastic scattering at high energy has the form (2.15) and (2.16), and the eikonal phase can be expressed in terms of the quasi-potential in the form

$$\delta(s,b)=\frac{1}{s}\int_{-\infty}^{\infty} V\left(s,\sqrt{b^2+z^2}\right)dz. \tag{2.23}$$

This representation of the amplitude is asymptotically exact. However, to draw any conclusions about the scattering amplitude, we must know the energy-dependent quasi-potential. In describing elastic scattering at high energies, it is usual to use a purely imaginary quasi-potential of Gaussian type,[21,22] $V(s,t) = isg \exp \lambda t$, where $\lambda = c_1 + c_2 \ln s$. With this choice of the quasi-potential, the scattering amplitude is described by Eqs. (2.15), (2.16) and (2.21) and corresponds exactly to the sum of the graphs of Fig. 4, associated with elastic rescatterings by the Pomeranchuk pole. Smooth quasi-potentials, like rescatterings in the framework of complex angular momentum theory, lead[22] to an amplitude in the region of large $|t|$ which has the form $T(s,t) \sim \exp(-\sqrt{\alpha' t \ln s})$, with additional oscillations.[23] It is significant that the behavior of the amplitude in the region of small $|t|$ determines its properties in a large region of momentum transfers.

4) The quark model. The interactions of hadrons at high energy are also described by models in which a hadron is regarded as a composite particle. The most popular such model is the quark model. In this model, the proton consists of three quarks, bosons consist of a quark and an antiquark, and the amplitude for the scattering of hadrons is expressed in terms of the amplitudes for the scattering of quarks, which makes it possible to interrelate the amplitudes for various processes.[24] Adopting the hypothesis that the quark interactions are additive, we can, for example, obtain relations of the following type:

$$\left.\begin{aligned}(\sigma_t^{\bar{p}p}-\sigma_t^{pp})-(\sigma_t^{\bar{p}n}-\sigma_t^{pn})&=\sigma_t^{\pi^-p}-\sigma_t^{\pi^+p},\\ (\sigma_t^{K^-p}-\sigma_t^{K^+p})-(\sigma_t^{K^-n}-\sigma_t^{K^+n})&=\sigma_t^{\pi^-p}-\sigma_t^{\pi^+p},\\ \sigma_t^{\pi N}&=\frac{2}{3}\sigma_t^{NN}.\end{aligned}\right\} \tag{2.24}$$

The quark model has recently been used not only to establish relations of the type (2.24), but also to determine the dependences of the amplitudes on s and t.

It is natural to expect that the internal structure of hadrons may show up in studying scattering at large momentum transfers $|t| \sim s \gg m^2$, since, by virtue of the uncertainty relation $\Delta p \cdot \Delta x \sim 1$, such processes correspond to an interaction at very small distances $x \sim |t|^{-1/2}$. A simple dimensional analysis of the amplitudes in the framework of the quark model[25] leads to the following expression for the differential cross sections for two-particle processes involving the scattering of high-energy particles at a fixed angle θ:

$$\frac{d\sigma}{dt}=F(\theta)\,s^{-m}, \tag{2.25}$$

$$m=\sum_{i=1}^{4} n_i-2, \tag{2.26}$$

where n_i is the number of elementary constituents (quarks or antiquarks) in particle i. According to (2.26), we have m = 10 for elastic pp scattering, and m = 8 for elastic πN and KN scattering.

The power-law fall-off (2.25) of the cross sections for two-particle processes with increasing energy is characteristic of most models in which the scattering of hadrons with large momentum transfers is due to the interaction or exchange of elementary constituents (partons or quarks), although the value of m is strongly dependent on the form of the model which is adopted.

2.2. Experimental Methods of Studying Elastic Scattering

Owing to the large drop in the cross sections when measurements are made in a large range of t and the diversity of requirements on the apparatus determined by the physical problem, contemporary experiments on elastic scattering can be divided into several types: interference measurements for $10^{-4} \leq -t \leq 10^{-2}$ (GeV/c)^2, measurements within the diffraction peak ($-t < 0.5$ (GeV/c)^2), measurements in the region of large momentum transfers ($-t \sim u \sim s$, $\theta \sim 90°$), and the study of backward scattering.

a) Measurements of differential cross sections in the Coulomb-nuclear interference region. Interference measurements are characterized by exceptionally high demands on the angular resolution of the apparatus. It became possible to determine the phase of the elastic forward scattering amplitude at high energies only after the development of new measuring techniques which make it possible to detect scattering down to very low momentum transfers $-t \sim 10^{-3}$ (GeV/c)^2, where the cross section is no longer determined only by the nuclear interaction, but depends also on Coulomb scattering and the effect of its interference with the nuclear scattering.

It is possible to study the elastic scattering of particles by detecting either the fast scattered particle or the recoil particle. In the first case (if only the fast scat-

tered particle is detected), technical difficulties occur in the high-energy region, owing to the decrease in the average scattering angle of the particles with increasing energy. It is well known that the average momentum transfer p_t in the elastic scattering of particles changes little with increasing energy, so that the average scattering angle $\varphi \sim p_t/p$ decreases in proportion to the momentum of the scattering particles p. Accordingly, the requirements on the angular (and energy) resolution of the experimental apparatus grow in proportion to the momentum.

Such difficulties do not occur if elastic scattering is studied by means of the recoil particle. However, the recoil particle has a low energy in small-angle scattering, so that its initial velocity and direction are modified by the interaction with the matter of the target, thus hindering the separation of elastic events according to the angle-momentum relation. This limitation is not a fundamental one, and methods have been found of putting such an experimental scheme into practice. In the early 1960s, methods of studying the interference region by means of the recoil particle were developed in Dubna and applied in experiments on pp and πp scattering;[26] these methods made use of targets of very low density and also guaranteed a high rate of collecting statistics and a high resolution in the momentum transfer.

The interference experiments on pp scattering exploited the ability of cyclic accelerators to maintain in orbit protons which have passed through a target, provided that the loss of energy in the target does not exceed the value allowed by the phase stability condition. With the realization of the regime of multiple passages of the beam through the target, it is possible to substantially reduce its dimensions. As a result, the conditions of the experiment are improved: the Coulomb scattering of the protons in the target leads to a minimum (which makes it possible to study the region of small momentum transfers); the ionization losses of energy by the recoil protons and the probability of their interaction in the target become negligibly small; in addition to the gain in resolution and intensity, there is a significant improvement in the ratio of the effect to the background from the accelerator.

The first experiments[27] were performed on the JINR synchrophasotron, which is an accelerator with weak focusing. A significant development of this technique was made in experiments carried out on the accelerators at Serpukhov[28,29] and Batavia (U.S.A.).[30,31] The recoil protons were detected by a multi-channel spectrometer with semiconductor detectors in on-line operation with a computer. The basic scheme of the experimental arrangement is shown in Fig. 5.

The smaller dimensions of the beam in comparison with the weak-focusing accelerator made it possible to use as the target a gaseous hydrogen jet with a density $\sim 10^{17}$ protons per cm^2, thereby eliminating almost completely the rescattering of the recoil proton by the matter of the target. In spite of this small quantity of matter in the target, the principle of multiple passage of the proton beam through the target guarantees that the statistics of elastic events are collected at a high rate ($\sim 10^6$ events per hour), which is at the present time a record level in experiments on elastic scattering. It can be seen from the example of these experiments that the development of electronics and the application of computers have altered the traditional situation in high-

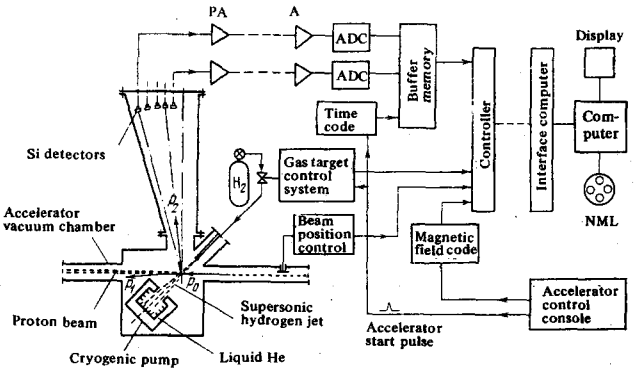

FIG. 5. Scheme of the spectrometer with semiconductor detectors for the study of elastic pp scattering at small angles, used in the experiments at the Serpukhov [29] and Batavia [30] accelerators. The spectrometer contains 12 spectrometric channels, each of which consists of a semiconductor detector, a pre-amplifier (PA), a spectrometric amplifier (A) and an analog-digital converter (ADC). The target is a supersonic hydrogen jet which intersects the internal beam of the accelerator.

energy physics in which the number of detected events had a decisive effect on the size of the errors in the measurements. In experiments with such high statistical accuracy, it becomes more important to consider methodological errors in the measurements (the stability of the detecting devices, the correctness of the allowance for corrections due to the geometry of the experiment, the resolution, counting losses, etc.) and theoretical ambiguities in the procedure of analyzing the experimental data (such as those due to poor accuracy of calculations of the electromagnetic corrections to the elastic scattering amplitude).

The thin-target technique is not effective in extracted beams of particles when it is not possible to ensure the condition of multiple passage of the particles through the target. To measure the cross section for the scattering of pions with small momentum transfers (30 MeV/c $< p_t <$ 100 MeV/c), another method was developed,[32] in which the functions of the gaseous hydrogen target and the detector of the slow recoil particles were performed by one and the same device. To distinguish the elastic events according to their kinematics, measurements were made of the proton momentum and its angle with respect to the direction of the meson beam at the point of interaction. By measuring the path length of the recoil proton, a resolution in t better than 10^{-3} (GeV/c)^2 was achieved.

Elastic scattering has been studied in a number of experiments by the technique of spectrometry of the angles and momenta of the scattered pions by means of magnetic spectrometers. Experiments at Brookhaven[33] and at Serpukhov[34] made use of hodoscope systems as coordinate detectors, which were used to measure the scattering angles and the angles of deflection of the particles by an analyzing magnet. Experiments on proton-proton scattering carried out at CERN and at the Rutherford Laboratory (England),[35] as well as experiments on πp scattering at Dubna,[36] used spark chambers instead of scintillation hodoscopes. Because of the large dead time of spark chambers, it is necessary to use fast (nanosecond) logical systems for the preliminary selection of scattering events.[36]

b) The procedure of determining the polarization parameters. The polarization parameters (1.10)–(1.12) are determined in experiments involving the scattering

of particles by polarized targets. The targets which are usually employed are organic compounds containing a large quantity of hydrogen (such as butanol, $C_4H_{10}O$, or ethylene glycol, $C_2H_6O_2$), cooled to a temperature $\sim 0.3\,^\circ$K. At such low temperatures the polarization of the hydrogen nuclei in the target can attain values 70–90%.[37]

The polarization P in elastic scattering is determined by measuring the left-right asymmetry of the scattering in the plane perpendicular to the direction of the polarization of the target. To determine the spin rotation parameters R and A, it is necessary to analyze the polarization $\mathbf{P}_f$ of the recoil proton after the scattering under conditions in which the polarization $\mathbf{P}_i$ of the target lies in the scattering plane (Fig. 6). The relations between the components of the initial polarization $\mathbf{P}_i$ and the final polarization $\mathbf{P}_f$ for πp scattering can be written in the form

$$\left.\begin{aligned} u &= \mathbf{P}_f[\mathbf{k}_i\times\mathbf{n}] = \{R\mathbf{P}_i[\mathbf{k}_i\times\mathbf{n}] - A\mathbf{P}_i\mathbf{k}_i\}(1+P\mathbf{P}_i\mathbf{n})^{-1},\\ v &= \mathbf{P}_f\mathbf{k}_p = \{R\mathbf{P}_i\mathbf{k}_i + A\mathbf{P}_i[\mathbf{k}_i\times\mathbf{n}]\}(1+P\mathbf{P}_i\mathbf{n})^{-1},\\ w &= (P+\mathbf{P}_i\mathbf{n})(1+P\mathbf{P}_i\mathbf{n})^{-1}; \end{aligned}\right\} \quad (2.27)$$

here $\mathbf{n} = (\mathbf{k}_i\times\mathbf{k}_f)/|\mathbf{k}_i\times\mathbf{k}_f|$, and $\mathbf{k}_i$, $\mathbf{k}_f$ and $\mathbf{k}_p$ are unit vectors in the laboratory coordinate system directed along the momenta of the incident pion, the scattered pion and the recoil proton, respectively. The differential cross section and the polarization parameters are in turn related to the scattering amplitudes by Eqs. (1.9)–(1.12). It can be seen from Fig. 6 and Eqs. (2.27) that a determination of the parameter A(R) requires an analysis of the component of the polarization of the recoil proton u under conditions in which the target is polarized in the direction of $\mathbf{k}_i$ (perpendicular to $\mathbf{k}_i$). This component of polarization is determined by measuring the azimuthal distribution of recoil protons scattered by the target-analyzer (carbon). In addition to the detection of the recoil proton, it is also necessary to detect the scattered pion in order to separate the events on hydrogen from the background of reactions on the nuclei of the target. For methodological reasons, the range of momentum transfers which is studied is bounded below by $-t \leq 0.2$ $(\text{GeV}/c)^2$.

c) The study of elastic scattering in a wide range of momentum transfers. In going from the interference region to the region of large momentum transfers, there is a rapid growth in the path length of the recoil particles (and the cross sections fall off almost exponentially), and it becomes possible (and, owing to the reduction in the cross section, even necessary) to make use of two spectrometers for the simultaneous detection of both particles.

An example of an experimental arrangement for the study of scattering in a wide range of values of t is the CERN magnetic spectrometer,[38] which has been used to study the elastic scattering of pions, kaons, protons and antiprotons by protons at 5 GeV/c. The spectrometer (Fig. 7) incorporates the following elements: scintillation hodoscopes (H_i), which determine the direction of the incoming particles with an accuracy ± 0.8 mrad; threshold Cerenkov counters (C_i), which distinguish pions, kaons and nucleons from the incident beam of particles; scintillation counters (S_i) and veto counters (V_i), which eliminate the halo of the beam and the particles which have passed through the target without interacting; and two arms of a spectrometer consisting of a set of counters that determine the operative aperture of each arm, an analyzing magnet and telescopes of spark chambers (W_i). This system detects particles scattered within the range of laboratory angles from 4 to $\sim 180°$ (98% of the available interval in t is covered in the case of Kp scattering). With an intensity of the incident beam equal to $\sim 5\times 10^5$ particles per cycle of acceleration, the apparatus detected ~ 10 events per cycle which satisfied the trigger criteria. The information from all the counters and chambers was fed into a computer for subsequent analysis. The total number of useful events for each of the studied reactions was 10^4–10^5, and the measured differential cross sections varied in the range from 10 to 10^{-5} mb/$(\text{GeV}/c)^2$.

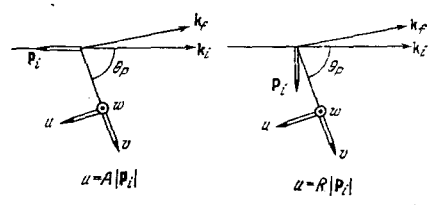

FIG. 6. Definition of the parameters P, R and A in experiments using a polarized target.

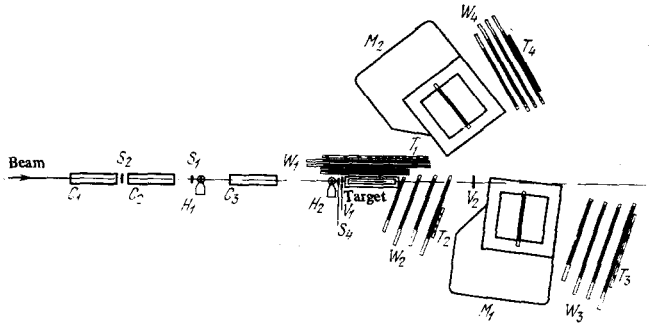

FIG. 7. Scheme of the magnetic spectrometer for studying the elastic scattering of hadrons in a wide range of momentum transfers [38]

This arrangement is typical for high-energy physics. Wide-aperture high-speed detectors of charged particles with a spatial resolution of the order of a fraction of a millimeter operate on-line with a computer, providing a high rate of collection and analysis of experimental information.

3. EXPERIMENTAL RESULTS

3.1. The Amplitudes for Forward Elastic Scattering of Hadrons

a) The imaginary part of the amplitude. By virtue of the optical theorem (2.2), the total cross sections determine the imaginary part of the elastic scattering amplitude for t = 0. In the case of NN scattering, the expression (2.2) applies to the spin-averaged interaction. In Fig. 8 we show the data on the total cross sections in the region of high energies $E > 5$ GeV, where structure in the dependence of $\sigma_t(E)$ due to s-channel resonances is no longer seen. It has been established from measurements of the total cross sections for $\pi^\pm p$, $K^\pm p$, pp and $\bar{p}p$ interactions up to 30 GeV that these cross sections depend on a power of the energy:

$$\sigma_t = \sigma_\infty + \frac{a}{p^m}. \quad (3.1)$$

An important result of the high-precision experiments performed at Serpukhov[39] was the observation that the

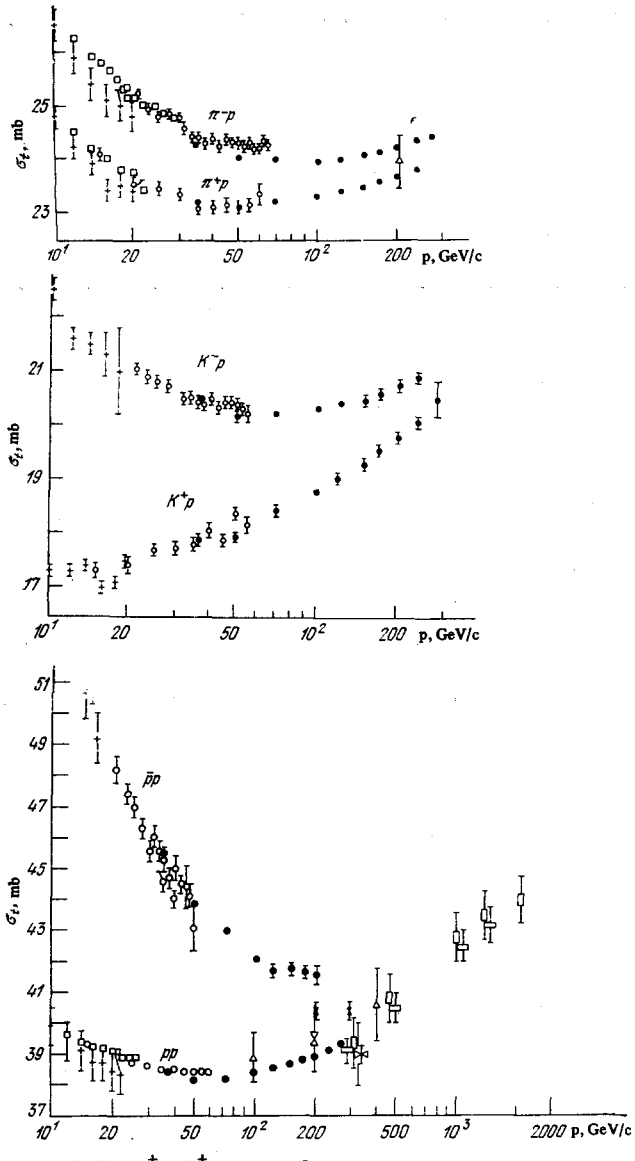

FIG. 8. The $\pi^{\pm}$p, $K^{\pm}$p, pp and $\bar{p}$p total interaction cross sections [39-41,43].

extrapolation of such a dependence to higher energies is unsound. It was found that the total cross sections for pp, $\pi^{\pm}$p and K^-p interactions remain practically constant in the energy region 30–50 GeV (for example, for π^-p and K^-p interactions, the total cross sections can be approximated by straight lines whose slopes have the values -0.004 ± 0.004 mb/(GeV/c) and -0.007 ± 0.004 mb/(GeV/c), respectively).

An even more significant result of the Serpukhov experiments is the observation of a growth in the total cross section for the K^+p system. Measurements of the total cross sections using the colliding beams at CERN (ISR)[40,41] up to s = 2800 GeV^2 (equivalent to a momentum p = 1500 GeV/c in the laboratory coordinate system) have demonstrated that the total cross section also rises in the case of the pp system. Qualitatively, such a behavior of the total cross sections had been predicted by complex angular momentum theory with allowance for cuts.[19] However, it is significant that the effect of the growth of the total cross sections was found to be unexpectedly large (of order 10% when $\sqrt{s}$ increases from 23 to 53 GeV) and showed up at energies much lower than expected (see Fig. 8). Experiments with cosmic rays have also indicated that nucleon-nucleus cross sections rise with energy.[42] It should be noted, however, that the results of [42] have evoked lively discussion.

Recent measurements of the total cross sections for $\pi^{\pm}$, $K^{\pm}$ and $\bar{p}$ interactions with hydrogen and deuterium at Batavia[43] confirm that the phenomena of rising cross sections is universal. A growth has not yet been established for the $\bar{p}p$ interaction, but the trend in the behavior of $\sigma_t^{\bar{p}p}(E)$ corresponds to the universal picture (the rate of fall-off of $\sigma_t(\bar{p}p)$ is slowing down).

The growth of the total pp cross section in the ISR energy region is described by the dependence[40]

$$\sigma_t = a_0 + a_1 \left(\ln \frac{s}{s_0}\right)^{\nu}, \tag{3.2}$$

where $\nu = 1.8 \pm 0.4$ (such an energy dependence of the imaginary part of the scattering amplitude with $\nu \leq 2$ is consistent with the Froissart bound (2.12)).

The differences between the total interaction cross sections for particles and antiparticles decrease with energy according to the power law

$$\Delta\sigma = \frac{b}{p^n}, \tag{3.3}$$

which has been established within the large energy range $6 \leqslant E \leqslant 200$ GeV. The values of n at the energies of Serpukhov[44] and Batavia[43] are in mutual agreement and vary for different reactions from ~0.4 to ~0.6. For the Kp system, the law of decrease of the difference of cross sections has been established both in measurements of the total cross sections for charged kaons and in experiments to measure the regeneration amplitude of neutral kaons in hydrogen, which is proportional to the difference of cross sections:[45]

$$\frac{2}{s} \operatorname{Im} T(K_L^0 \to K_S^0) = \sigma_t(K^0 p) - \sigma_t(\bar{K}^0 p) = \Delta\sigma_t. \tag{3.4}$$

The foregoing information about the energy dependence of the difference of total cross sections indicates that the Pomeranchuk theorem concerning the asymptotic equality of the total cross sections for particles and antiparticles is consistent with the experimental data. The parametrization (3.3) can be explained in a natural way within the framework of complex angular momentum theory: all differences of total cross sections must decrease asymptotically according to a power law, since they are determined by the contributions of the secondary Regge trajectories ρ, ω and A_2. This is true (with an accuracy up to logarithmic terms) even if allowance is made for branch points:[4)]

$$\Delta\sigma = \sum_i \left(\frac{s_0}{s}\right)^{1-\alpha_i(0)} f\left(\ln \frac{s}{s_0}\right). \tag{3.5}$$

b) Real part of the amplitude. We shall give here experimental data on the real parts of the amplitudes for elastic scattering of mesons and protons by protons. These data are obtained by analyzing differential cross sections in the Coulomb interference region. To determine the real part of the forward elastic scattering amplitude, the differential cross sections measured up to $|t| \approx 4 \times 10^{-4}$ (GeV/c)^2 were approximated by the formula

[4)] At the available energies, it proves to be quite important to allow for the logarithmic dependence on s due to the moving branch points. Consequently, the values of n which are found from experiment should be somewhat different from the actual values of $1 - \alpha_i(0)$ determined, for example, from the spectrum of resonances.

$$\frac{d\sigma}{dt} = \frac{1}{64\pi p^2 s} |T_C(1+2i\eta) + (\rho + i)\,\mathrm{Im}\,T|^2, \qquad (3.6)$$

in which $T = (\rho + i)\,\mathrm{Im}T$ is the hadronic scattering amplitude (in the spinless approximation), $T_C = 16\pi p\sqrt{s}\,e^2 \times F(t)/tv$ is the Coulomb scattering amplitude, e and v are the charge and velocity of the particles, F(t) is the electromagnetic form factor of the proton, and $\eta = -(e^2/v)\ln(b'\sqrt{|t|})$ is the shift in phase of the nuclear and Coulomb amplitudes, which has been calculated in [46] (the value of b′ is determined by the slope parameter B of the diffraction peak and the electromagnetic radii of the scattering particles). The representation of ImT(t) in the form of an exponential, Eq. (1.4), is valid for small momentum transfers |t|.

1) pp scattering. Elastic proton-proton scattering has aroused particular interest in recent years, since the process of pp scattering has been studied at the highest available accelerator energies ($s \sim 3000$ GeV^2) and therefore provides the most interesting information about the asymptotic behavior of the scattering amplitude.

The first measurements of the ratio of the real to imaginary part of the amplitude by means of the interference method were made in Dubna in 1963.[27] This experiment showed that, for pp scattering in the energy range 1–10 GeV, the real part of the amplitude is comparable with the imaginary part and is negative ($\rho = \mathrm{Re}\,T/\mathrm{Im}\,T \approx -0.3$). These experiments were followed by similar measurements in other laboratories and dispersion-relation calculations of the real part of the amplitude for the high-energy region which had become experimentally accessible.[47,48] This initiated the realization of the program of testing the basic principles of the theory by using dispersion relations to compare the experimental data on total cross sections with the results of measurements of the real part of the amplitude.

In Fig. 9 we show how the measured values of ρ(pp) compare with calculations based on dispersion relations. In the energy range 1–500 GeV, the experimental values of ρ in pp scattering obtained using the accelerators at Dubna,[51,52] Serpukhov,[29] CERN,[35,53] Brookhaven[33] and Batavia[31] are in qualitative agreement with the dispersion calculations. A quantitative comparison in the case of the pp interaction is complicated by two ambiguities, whose effect, however, becomes smaller with increasing energy. Calculations of the real parts of the pp amplitude at low energies are affected to a great extent by the unphysical region, while analyses of interference data require allowance for the spin-spin interaction. The contribution of the unphysical region to the dispersion integral is determined by comparing the dispersion calculations with the results of phase-shift analyses of pp scattering at low energies; the magnitude of this contribution falls off with energy[47] like $\sim E^{-1}$ and is no more than 10% at $E \approx 10$ GeV. Studies of the interactions of protons in pure spin states[54] and estimates of spin effects in interference experiments[52,55] show that these effects also have a small influence on the results of analyses of cross sections in the Coulomb-nuclear interference region at high energies.

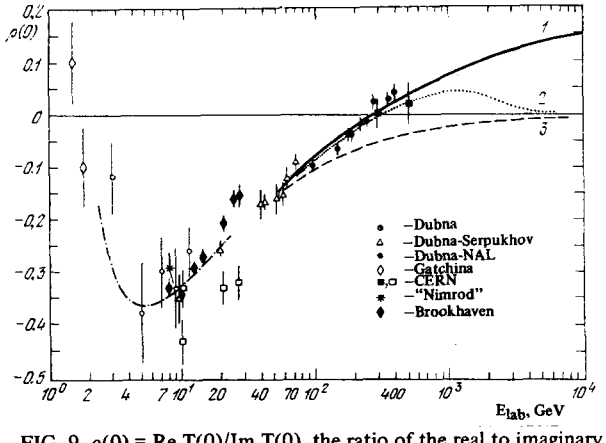

FIG. 9. $\rho(0) = \mathrm{Re}\,T(0)/\mathrm{Im}\,T(0)$, the ratio of the real to imaginary part of the amplitude in elastic pp forward scatter [29,31,33,35,49,51,53].

The theory imposes a number of restrictions on the behavior of the elastic scattering amplitude. In particular, it has been established[56–58] that the sign of the real part of the amplitude at high energies is directly related to the asymptotic form of the total cross sections:

$$\lim_{s\to\infty} \rho \sim \frac{1}{\sigma_t}\frac{d\sigma_t}{d\ln s}. \qquad (3.7)$$

Consequently, after the appearance of the first indications of a growth in the total cross section for the pp interaction at high energies, there arose the problem of studying the predicted change in the energy dependence $\rho(s)$. Recent data obtained using the colliding beams at CERN[53] and in the Soviet-American experiment at the Fermilab accelerator[31] have shown that the real part of the amplitude changes sign (becomes positive) at E ~ 280 GeV. The change in sign of the real part of the amplitude and the growth of the total cross section for pp scattering are mutually consistent effects.

An important feature of the dispersion relations for forward scattering is the sensitivity of the calculated values of the real part of the amplitude to the asymptotic behavior of the total cross sections. Because of this, measurements of the real parts of the amplitudes near the upper limit of the accessible energy range may provide a good test of the behavior of the total cross sections beyond this limit.[59] However, it is obvious that the further we want to see beyond the available energy range, the higher the accuracy with which the real part of the amplitude must be measured. The results of [31], in which measurements were made with an accuracy $\Delta\rho = 0.01$–0.015, are clearly incompatible with the hypothesis that the total cross sections fall off monotonically towards a constant value: in this case, the real part of the amplitude would have to remain negative at all energies (curve 3 in Fig. 9). The assumption that the total cross section rises like $\sim \ln^2 s$ and then tends to a constant at E ~ 2000 GeV is not well borne out (curve 2 in Fig. 9). The agreement with a parametrization of the total cross section in the form $\sigma_t = a_0 + a_1[\ln(s/s_0)]$ is more satisfactory (curve 1 in Fig. 9; the values of the constants a_0, a_1, s_0 and ν are given in [60]). However, the extent to which the energy dependence of ρ(pp) is in agreement with the dispersion predictions is improved by assuming a more rapid law of growth of the total cross section than that which is proposed in [60] and which is usually quoted (to bring the theoretical and experimental results into agreement, the authors of [61] use $a_1 = 0.77$ instead of $a_1 = 0.49$ [60]).

2) K^+p scattering. No accurate interference measurements of K^+p scattering have been made by the electronic technique in the range of energies above 3 GeV. The data

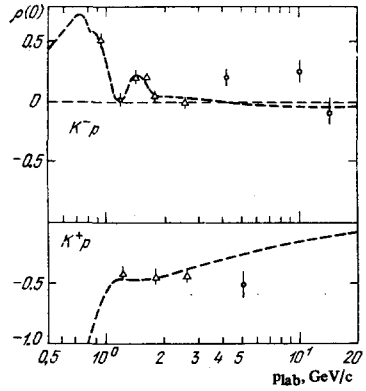

FIG. 10. $\rho(0)$ in elastic $K^{\pm}p$ scattering [62-64]. We show only the results of interference measurements. The dispersion curves are calculated under the assumption that the $K^{\pm}p$ total cross sections have the asymptotic value $\sigma_{\pm}(\infty) = 19.2$ mb [64].

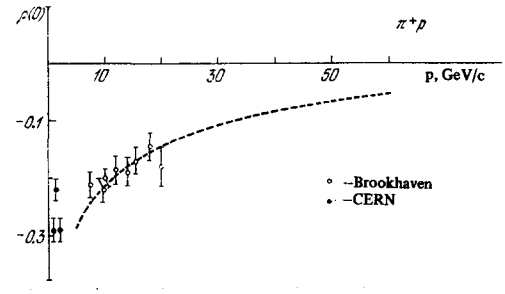

FIG. 11. $\rho(0)$ in elastic π^+p scattering [33,64]. The dispersion curve [50] takes into account the latest data on the rising total cross sections for the $\pi^{\pm}p$ interaction [43].

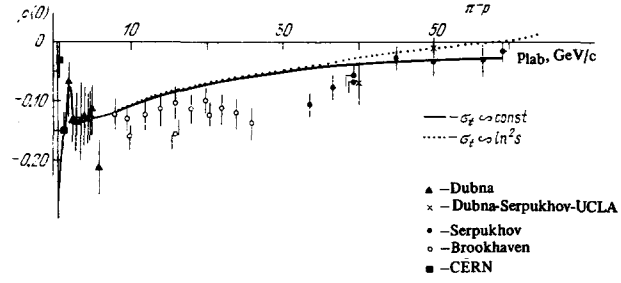

FIG. 12. $\rho(0)$ in elastic π^-p scattering [32,33,64,69-71]. The dispersion curves are calculated under two different assumptions about the behavior of the total cross sections for the $\pi^{\pm}p$ interaction [4,50] for $p > 60$ GeV/c. (The dotted curve takes into account the growth of the total cross sections [43].)

on K^+p and K^-p scattering shown in Fig. 10 were obtained by using a liquid hydrogen chamber exposed to the separated beams at CERN[62,63] and do not include the angular region in which the interference effect is appreciable. For this reason, these results have a lower accuracy than in the case of pp or πp scattering.

The first direct measurement of $K^{\pm}p$ forward scattering which included the interference region for values $0.008 \leq |t| \leq 0.1$ (GeV/c)^2 was made at CERN at momenta between 0.9 and 2.6 GeV/c, using a non-magnetic spectrometer with proportional chambers.[64] The authors of this experimental paper made use of the available data on phase-shift analyses of Kp scattering to estimate the magnitude of the spin-flip term[5] in the scattering amplitude and found that this term is less than 0.2%. The results of this experiment were used to improve the accuracy of the values of the ΛKN and ΣKN coupling constants, a knowledge of which is needed to calculate the real parts of the $K^{\pm}p$ forward scattering amplitudes on the basis of dispersion theory. The dispersion curves obtained in [64] provide a satisfactory description of the experimental data for $p < 3$ GeV/c, but it is not possible to obtain a consistent simultaneous description of the existing data on K^-p and K^+p scattering in the region of higher energies (see Fig. 10).

In the case of kaon-proton scattering, information on the real parts of the $K^{\pm}N$ amplitudes can be obtained not only by direct measurements of the Coulomb interference, but also by measuring the $K_L^0 \to K_S^0$ regeneration. Regeneration experiments involve measurements of the crossing-odd amplitudes

$$\begin{aligned} f(K^-p \to K^-p) - f(K^+p \to K^+p) &= -2f(K_L^0 n \to K_S^0 n), \\ f(K^-n \to K^-n) - f(K^+n \to K^+n) &= -2f(K_L^0 p \to K_S^0 p). \end{aligned} \tag{3.8}$$

Experimental data on the modulus and phase of the regeneration amplitude in hydrogen[45,65,66] and deuterium[67,68] can be used to obtain the real part of the regeneration amplitude for the neutron, $\mathrm{Re}\,(K_L^0 n \to K_S^0 n)$, and to compare it with the difference between the real parts of the $K^{\pm}p$ amplitudes.[68] Such a comparison reveals a significant discrepancy between the results. Thus, we require a further refinement in the experimental status of kaon-proton scattering in the range of high energies which is currently accessible to accelerators. The present status of the test of dispersion relations is clearly unsatisfactory in this case.

3) $\pi^{\pm}p$ scattering. A year ago, the only interference measurements in πp scattering were the data of two experimental groups at Brookhaven[33] (U.S.A.) and at Dubna.[32,69] These results have now been supplemented by data obtained at energies above 30 GeV/c at Serpukhov[70,71] and results at CERN for $E \leq 2$ BeV/c.[72] Figures 11 and 12 show a compilation of experimental data on $\pi^{\pm}p$ scattering in the momentum range from 1 to 60 GeV/c.

The most direct test of the basic principles of local field theory can be made by comparing the data on pion-nucleon forward scattering with the predictions of dispersion calculations. In fact, in contrast with the case of pp or Kp scattering, the dispersion relations for πp scattering at zero angle contain no unobservable quantities and express the real part of the elastic forward scattering amplitude in terms of data on the total $\pi^{\pm}p$ cross sections and constants which can be determined from experiments on low-energy scattering. A comparison of the measured values of $\rho(E)$ with those calculated from dispersion relations reveals that the results are in good agreement with the calculations in the range of energies below 8 GeV/c. The absence of discrepancies in the region in which resonance contributions have a strong effect on the behavior of the total cross sections for $\pi^{\pm}p$ scattering ($p < 2.5$ GeV/c) and in which the value of $\rho(E)$ is varying rapidly indicates that there is good general self-consistency of the data on the pion-nucleon interaction in the region of low and intermediate energies.

At high energies, when the experimental data are compared with dispersion calculations (the dotted curve in Fig. 12) which take into account the experimentally established growth of the total $\pi^{\pm}p$ cross sections above 100 GeV,[50] it is found that the data of the Brookhaven group[33] on π^-p scattering (Fig. 12) deviate more and more from the calculated dependence $\rho(E)$ with increasing energy. A discrepancy between the measured and

[5]The contribution of the process involving a reversal of the spin.

calculated values of ρ in this energy region has also been found in [70,71]. At the same time, the data on π^+p scattering (Fig. 11) are in satisfactory agreement with the dispersion calculations. To understand this contradictory situation, we require further precision measurements of $\rho(E)$, particularly in the range $10 \leqslant E \leqslant 60$ GeV, where the theoretical predictions of $\rho(E)$ are quite reliable because good measurements of the total cross sections have been made up to 200 GeV.

As to the possible violation of the dispersion relations and an estimate of the dimensions l_0 of a hypothetical region of acausality,[73,74] it should be noted that there is a need for not only reliable data on the modulus and phase of the forward πN scattering amplitude, but also a sufficiently consistent technique by which a fundamental length l_0 is introduced in the theory and the effects associated with it are estimated. The current experimental data on πp and pp scattering do not provide any indications for the existence of an acausal region comparable with the range of the strong interactions.

A number of experiments have revealed a discrepancy between the values of $(d\sigma/dt)_{t=0}$ obtained by extrapolating the data to t = 0 and the "optical point," and this has initiated a discussion concerning the possibility of a violation of the optical theorem in hadronic interactions.[75,76] This discrepancy may be attributed to an inaccuracy of an extrapolation from the range of values $|t| > 0.1$ $(GeV/c)^2$ which is based on the assumption that the peak has an exponential form. In this sense, tests of the optical theorem (unitarity) are related to the problem (considered below) of the form of the diffraction peak for $|t| < 0.1$ $(GeV/c)^2$ and require very accurate measurements of the differential cross sections in this region of momentum transfers. An analysis of the entire set of experimental data referring to this problem indicates that there are no serious signs of a breakdown of the optical theorem, since the existing discrepancies are always of the order of the systematic errors and the ambiguities in the extrapolation.[76]

3.2. Slopes of the Diffraction Peaks

In the region of small momentum transfers $|t| < 0.1$ $(GeV/c)^2$, the differential cross sections for elastic processes can be approximated by an exponential form $\exp(Bt)$. The slope parameter $B(s,t)$, along with the total cross section and the phase of the scattering amplitude, is a primary characteristic of a process, since it plays a major role in the theory of hadronic interactions. We recall, for example, that the experimental data on the energy dependence of the parameter $B(s)$ was the first touchstone for testing the Regge-pole model.

At high energies, the value of B lies in the range 8–12 $(GeV/c)^{-2}$ for all measured processes of elastic scattering of hadrons.

In general, the value of B depends on the nature of the scattering particles, their energy and the interval of t in which the measurements are made. For all reactions which have been studied, the slope increases as the magnitude of the momentum transfer becomes smaller. Measurements of $B(s,t)$ at small $|t|$ are of theoretical interest in most cases. We shall therefore generally confine our discussion to the region of small momentum transfers, $|t| \leq 0.1$ $(GeV/c)^2$.

a) **Shrinkage of the peaks.** The experimental information about the slope parameter in the region of small momentum transfers is rather poor: it has generally been obtained using the same experimental arrangements that were used to carry out interference measurements of the phase of the forward scattering amplitude. The most information has been obtained in the case of proton-proton scattering, where the effect of the growth in the slope parameter with increasing energy—the shrinkage of the diffraction peak—was first observed.

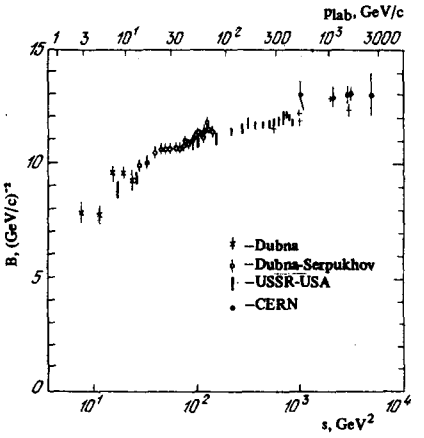

FIG. 13. The slope parameter B for the diffraction peak in elastic pp scattering for $-t \lesssim 0.1$ $(GeV/c)^2$ [28,30,33,35,51,77,78].

Figure 13 shows the existing experimental data on the slope of the peak in pp scattering[28,30,35,51,77,78] in the energy range $4.5 < s < 3600$ GeV^2. The experiment of the Dubna-Serpukhov group[28] involved a measurement of the dependence of the slope parameter for pp scattering in the momentum range 10–70 GeV/c. The energy dependence of the slope parameter for pp scattering in the range $-t \leqslant 0.1$ $(GeV/c)^2$ is described by the logarithmic behavior

$$B(s) = B_0 + 2\alpha' \ln \frac{s}{s_0}. \qquad (3.9)$$

The shrinkage of the peak is characterized by the parameter α', whose value for this energy range is $\alpha' = 0.41 \pm 0.06$ $(GeV/c)^{-2}$. Similar measurements performed by the Soviet-American group at Batavia[30] showed that the peak in elastic pp scattering continues to shrink as the energy of the scattering protons increases, although possibly more slowly. In the energy range 50–400 GeV, $\alpha' = (0.278 \pm 0.024)$ $(GeV/c)^{-2}$. The conclusion that the rate of shrinkage is slowing down with increasing s is strengthened if one takes into account the data within the entire energy range starting with $s = 4.5$ GeV^2.

The information on the slope parameter for $\pi^\pm p$ scattering is shown in Fig. 14. It has been noted[79] that, if only small momentum transfers are considered (these are the data that were used in Fig. 14), then the slope of the peak is also found to grow with energy in the case of $\pi^\pm p$ scattering at energies above 3 GeV (the parameter B does not behave monotonically as a function of energy in the range $E < 3$ GeV, which is characterized by the presence of resonances in the πp system).

The preliminary results of experiments on $\pi^\pm p$, $K^\pm p$, pp and $\bar{p}p$ scattering performed in the neighboring interval $0.07 \leq -t \leq 0.3$ $(GeV/c)^2$ at Batavia,[80] as well as measurements made at Serpukhov,[81–84] also indicate that the parameter $B(s,t)$ is increasing with s (Fig. 15). (The case of $\bar{p}p$ scattering, where the peak is expanding with s, is an exception. However, there is still hope that

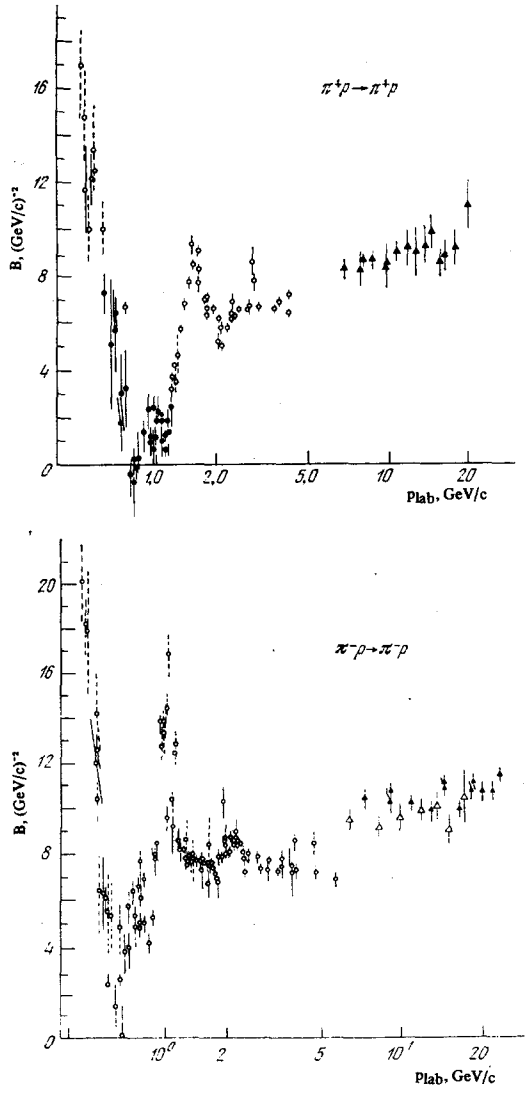

FIG. 14. The slope parameter B for $\pi^{\pm}$p scattering. The values of B for p > 5 GeV/c are determined for the interval $-t \leqslant 0.04$ (GeV/c)^2 [79].

this distinction will disappear at high energies, once the $\bar{p}p$ total cross section stops decreasing.)

We recall that it was assumed in the 1960s that there is no shrinkage of the peak for the πp system, whereas a very strong shrinkage was seen for energies $3 \leq E \leq 20$ GeV in the case of pp scattering. Now that a larger range of energies has been studied, the experimental picture is approaching a universal one. Our point of view has changed for two reasons: first, it has been found that the slope parameter depends on the value of t at which it is measured (see Sec. 3.2b), and it has become obvious that comparisons must be made within one and the same interval of t near t = 0; second, it was found that the rate of shrinkage of the proton peak has become much slower in going from the energies 3–30 GeV to the range 10–70 GeV (see Fig. 13).

It follows from the experiments performed in the energy range E ~ 10–100 GeV that the slopes of the diffraction peaks for the elastic scattering of protons, pions and kaons by protons increase not faster than ln s. There are no indications here of a possible violation of the asymptotic bound (2.13), namely $B(s) \leq \text{const} \cdot \ln^2 s$, which the axiomatic theory imposes on the energy dependence of the slope parameter.

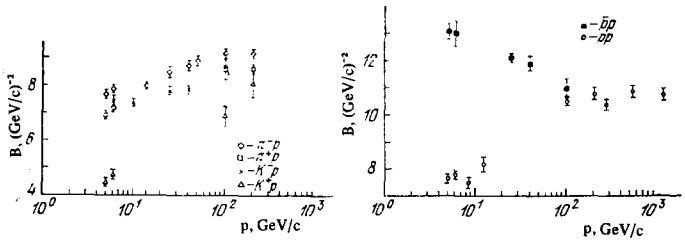

FIG. 15. The parameter B in $\pi^{\pm}$p, $K^{\pm}$p, pp and $\bar{p}$p scattering [80] for the interval $0.1 \leqslant -t \leqslant 0.3$ (GeV/c)^2.

But what is the asymptotic dependence of B(s)? From the experimental standpoint, this question has now been studied most thoroughly in the case of proton-proton scattering: high-precision experiments in the range of energies up to s ~ 750 GeV^2 using internal accelerator targets,[28–30] as well as data obtained using the colliding beams at CERN,[77,78] have made it possible to extend the range of the investigations up to energies corresponding to a momentum 1500 GeV/c in the laboratory coordinate system. Unfortunately, even in this case, we cannot distinguish between two possibilities: either the slope parameter continues to rise logarithmically as $s \to \infty$ in accordance with Eq. (3.9), or the growth of B(s) stops ($\alpha' \to 0$) as $s \to \infty$.

b) The slope of the peak as a function of the momentum transfer. In our discussion of the energy dependence of the parameter B(s) in the preceding subsection, the range of momentum transfers was limited to the small interval $0.01 \leq -t \leq 0.1$ (GeV/c)^2, in which the slope does not vary with t within the experimental accuracy. (It is only the absence of good experimental data near t ~ 0 for the processes of elastic scattering of pions, kaons and antiprotons which forced us to make use of information from a larger interval of t.) In this subsection we discuss the slope of the peak as a function of the momentum transfer; in other words, we consider the form of the differential cross sections within the diffraction peak. We extend the range of momentum transfers. We choose the upper limit $-t < 0.4$ (GeV/c)^2, so as to exclude the region of momentum transfers in which the curve for $d\sigma(t)/dt$ begins to exhibit structure, possibly associated with interference phenomena (see Fig. 16 and Sec. 3.4).

Until recently, an exponential with a linear t-dependence was used to parametrize the cross sections for elastic processes in this region of small momentum transfers. The motive for this choice was the optical model, in terms of which the angular dependence of the elastic scattering amplitudes is described by a formula of the type (2.17), which in the case of small momentum transfers corresponds to an exponential with a linear t-dependence, $d\sigma/dt \sim \exp(R^2 t/4)$.

With the appearance of sufficiently accurate experimental data on the scattering of protons, it has become clear that an exponential with a linear t-dependence is not in agreement with experiment, even in this narrow interval Δt near t = 0. First of all, it was shown[33,51,86] that the slopes of the peaks measured in the range $-t < 0.1$ (GeV/c)^2 are larger than those in the range $0.1 < -t < 0.3$ (GeV/c)^2. Subsequently, a single experiment[78] using the colliding beams at CERN showed directly that the slope changes near $-t \approx 0.1$ (GeV/c)^2 (Fig. 17). Recently, direct experimental evidence has been obtained that the slope also changes in π^-p scat-

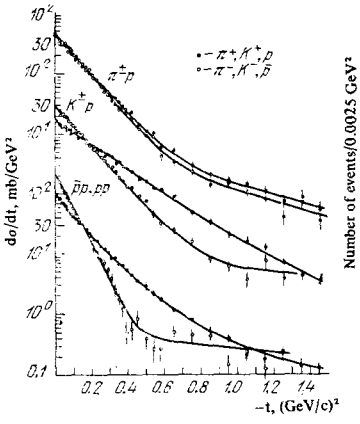

FIG. 16

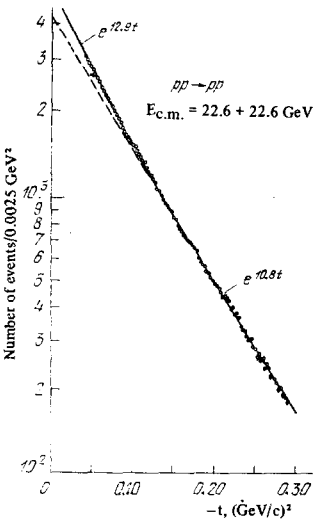

FIG. 17

FIG. 16. The diffraction peak in $\pi^{\pm}p$, $K^{\pm}p$, $\bar{p}p$ and pp scattering at p = 5 GeV/c [85].

FIG. 17. Measurement of the slope of the diffraction peak [78] in the region $-t \approx 0.12$ (GeV/c)².

tering (the experiments[87] were performed at 8 GeV) from $B = 8.19 \pm 0.19$ (GeV/c)$^{-2}$ for $0.02 < -t < 0.10$ (GeV/c)² to $B = 7.23 \pm 0.05$ (GeV/c)$^{-2}$ for $0.15 < -t < 0.5$ (GeV/c)². The effect of the change in slope is less pronounced for scattering of negatively charged kaons;[87] it is not observed in the case of antiproton scattering (the scattering of positively charged particles was not studied in this work). There is as yet no generally accepted explanation of this effect. By using the analytic properties of the scattering amplitudes,[88] it can be related to the effect of the structure of the nearby cuts on the scattering amplitude in the neighboring physical region, and this leads to a continuous growth of the slope of the peak as $t \to 0$. A parametrization of the differential cross sections which allows for the change of slope has been proposed in [89]

c) Comparison of dσ/dt for particles and antiparticles. As in the case of the total cross sections, the differential cross sections for elastic scattering of antiparticles ($d\sigma^-/dt$) and their logarithmic derivatives (B^-) at t = 0 exceed the analogous quantities ($d\sigma^+/dt$ and B^+) for the corresponding particles; but since $B^- > B^+$, the cross sections become equal at some $t = t_c$ (see Fig. 16; the curves for $d\sigma^-/dt$ and $d\sigma^+/dt$ cross—this is the so-called "cross-over phenomenon").

It is of interest to consider the energy dependence of the cross-over point, since this provides a sensitive test of a number of theoretical models. The difference between the differential cross sections is approximately proportional to Im $V_{\Delta\lambda=0}$, the imaginary part of the helicity-conserving amplitude corresponding to t-channel exchanges with the quantum numbers of the vector mesons:

$$\Delta\left(\frac{d\sigma}{dt}\right) = \frac{d\sigma^-}{dt} - \frac{d\sigma^+}{dt} \sim \operatorname{Im} V_{\Delta\lambda=0}.$$

In the geometric model,[90] this amplitude is proportional to the Bessel function of order zero:

$$\operatorname{Im} V_{\Delta\lambda=0} \sim J_0\left(R\sqrt{-t}\right),$$

so that t_c moves towards smaller |t| if the radius grows with increasing s. In the single-pole Regge model, the cross-over point is independent of the energy.

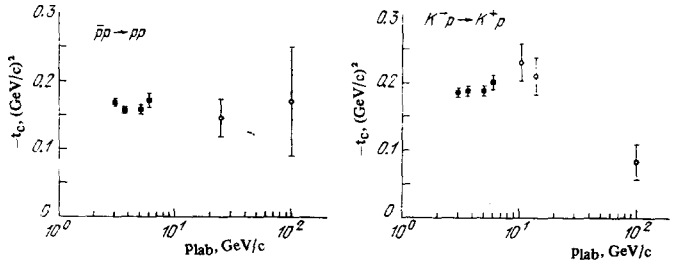

FIG. 18. Energy dependence of the position of the cross-over point [90]. The points for p < 10 GeV/c are the results of direct measurements. Above 10 GeV/c we show the values of t_c calculated from data on the total cross sections and the slope parameters for particles and antiparticles.

The experimental information on the energy dependence of the cross-over point t_c for kaon-proton and proton-proton scattering is shown in Fig. 18.[90] Unfortunately, owing to the small number of experiments and their poor accuracy, we cannot draw any definite conclusions at the present time.

3.3. Behavior of the Cross Sections in the Region $0.5 < -t < 3$ (GeV/c)²

In Fig. 1 we showed the differential cross sections for the elastic scattering of hadrons by protons at 5 GeV/c, measured by means of a double-arm spectrometer[38] within the wide range of momentum transfers $0.2 \leq -t \leq 8$ (GeV/c)². All the reactions except K^+p and pp scattering are characterized by the presence of structures in dσ/dt in the region of momentum transfers $0.5 \leqslant -t \leqslant 3$ GeV². This region is a transition region from the regime of scattering with small momentum transfers, which is described by Eqs. (2.17) and (2.19), to the regime of scattering with large momentum transfers, which may be related to the interaction of hypothetical particles that make up the structure of the nucleon. As can be seen drom Fig. 1, the t-dependence of dσ/dt in this transition region is not monotonic.

The fact that structures in dσ/dt occur for elastic pp, K^-p and $\pi^{\pm}p$ scattering but not in K^+p or pp scattering can be understood in the framework of dual models. In these models, the contributions of the secondary Regge poles (ω, P′, ρ, A_2) to the elastic K^+p and pp scattering amplitudes are real, since there are no known resonances in the "exotic" channels, namely K^+p and pp scattering. For energies < 5 GeV, these real contributions completely fill in the minima of dσ/dt, corresponding to the predominantly imaginary contribution of the vacuum singularity. At the same time, the contributions of the secondary poles to the $\bar{p}p$ and K^-p elastic scattering amplitudes are purely imaginary and lead to structure in the differential cross sections in addition to the main structure due to pomeron exchange. In other words, the structure of the amplitudes in dual models is largely due to the direct-channel resonances which are absent in K^+p and pp scattering but which are important in $\bar{p}p$, K^-p and $\pi^{\pm}p$ scattering.

The cross sections in the interval of momentum transfers $0.03 < -t < 0.8$ (GeV/c)² are frequently parametrized by an exponential with a quadratic t-dependence:

$$\frac{d\sigma}{dt} \sim \exp(Bt + ct^2). \qquad (3.10)$$

The parameter c which is artificially introduced in this formula takes into account the effects associated with the above-mentioned structure of the differential cross

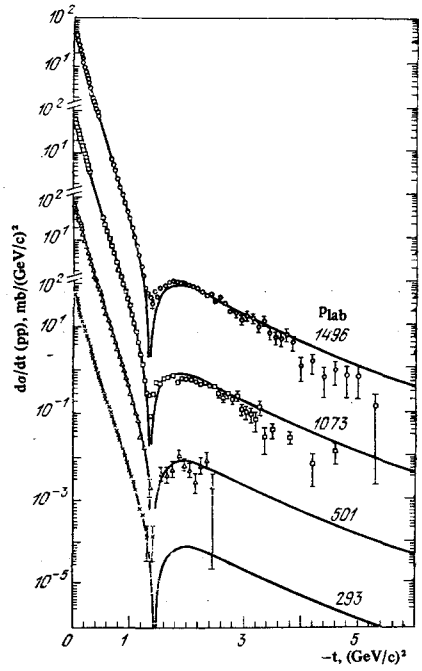

FIG. 19. Differential cross sections for elastic pp scattering at ISR energies [78]. The curves show the description of the differential cross sections in the model of geometric scaling [91].

sections, which can be described more naturally by a formula of the interference type:

$$\frac{d\sigma}{dt} \sim |a_1 \exp(B_1 t) + a_2 \exp(B_2 t)|^2. \qquad (3.11)$$

For energies 25–40 GeV, the adjustable coefficient c is found to have practically the same value for all particles,[82,84] namely $c \approx 2.5$ GeV^{-4}. The formula (3.10) is unsuitable at lower energies, where the structure in $d\sigma/dt$ is even more pronounced in this region of momentum transfers for $\pi^{\pm}p$, K^-p and $\bar{p}p$ scattering (see Fig. 16).

The role of the secondary singularities becomes less important as the energy increases, and at energies ~1000 GeV the character of the scattering begins to resemble a diffraction picture. In Fig. 19 we show the differential cross sections for elastic pp scattering at ISR energies.[78] A minimum in $d\sigma/dt$ at $|t| \sim 1.3$ GeV^2, as well as a second maximum at $|t| \sim 2$ GeV^2, are clearly seen. The measurements[92] show that the position of the minimum moves into the region of smaller $|t|$ as the energy increases, while the value of $d\sigma/dt$ at the second maximum rises. The total pp interaction cross section and the total cross section for elastic scattering rise in the same manner (by 10% in the energy range $400 < s < 3000$ GeV^2). This behavior is in accordance with the predictions of the model of "geometric scaling":[90,93]

$$\sigma_t \sim R^2, \qquad (3.12)$$

$$\sigma_{el} \sim R^2, \qquad (3.13)$$

$$d\sigma/dt \sim \sigma_t^2(s)\, F(R^2 t) = \sigma_t^2(s)\, F(\sigma_t t). \qquad (3.14)$$

According to (3.14), the position of the minimum in $d\sigma/dt$ falls off with energy like $-t_{min} \sim \sigma_t(s)^{-1}$, while the value of $d\sigma/dt$ at the second maximum rises with energy like $\sim \sigma_t(s)^2$.

It is assumed in the model of geometric scaling that the degree of "grayness" of a hadron is independent of the energy and that only the effective radius of interaction R(s) rises with increasing energy. (The partial-wave amplitude f(s, b), which is a function of both the impact parameter b and the energy s in the general case, depends only on the ratio b/R(s) in this model.) The condition

$$B \equiv \frac{d \ln (d\sigma/dt)}{dt} \sim \sigma_t \qquad (3.15)$$

which is implied by this assumption is poorly borne out by experiment: the slope of the peak rises more slowly than σ_t and σ_{el}.

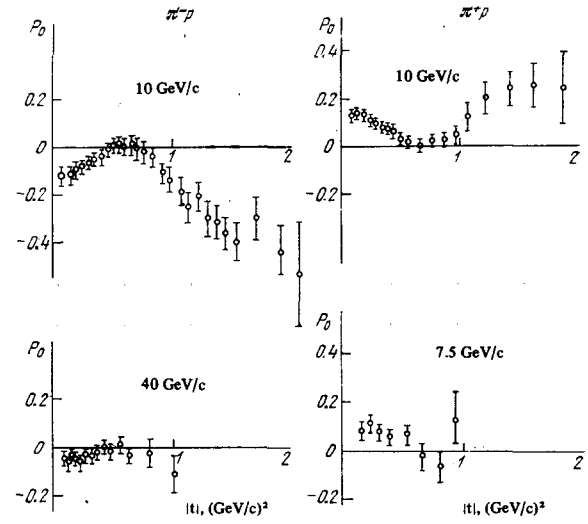

FIG. 20. The polarization in $\pi^{\pm}p$ scattering [94,95].

3.4. Polarization Measurements and the Reconstruction of the πN Scattering Amplitudes

There is now a significant accumulation of experimental information about the polarization in elastic scattering processes, although a set of data which is adequate for an amplitude analysis exists only for πp scattering at relatively low energies. The polarization data for $\pi^{\pm}p$ scattering are shown in Fig. 20. The characteristic dependence with a maximum in $P_-(t)$ at $-t \approx 0.6$ GeV^2 (where $P_-(t) = 0$) which is observed at energies ~10 GeV[94] is still present at p = 40 GeV/c (according to the results of a joint Soviet-French experiment using the IHEP accelerator),[95] although the absolute value of the polarization at p = 40 GeV/c has become smaller than the data at p = 14 GeV/c by almost a factor of two. It is of interest to observe that the polarization in the scattering of positively charged pions throughout the studied energy range is equal in magnitude but opposite in sign to the polarization in the reaction $\pi^-p \to \pi^-p$. The energy dependence of the polarization in π^+p scattering is shown in Fig. 21. Such a dependence of the polarization on a power of s is in agreement with the predictions of the Regge-pole model, in which the polarization is a result of the interference between the P pole and the secondary poles and should fall off like $s^{\alpha_\rho(t)-\alpha_P(t)}$.

At the energy 6 GeV, there exists experimental information[97] on the seven quantities $d\sigma_+/dt$, $d\sigma_-/dt$, $d\sigma_0/dt$, P_+, P_-, P_0 and R_-,[6)] where +, − and 0 refer to the pro-

[6)]The experimental status of the measurements of P_0 at energies 5-6 GeV remains somewhat unclear at the present time. The CERN-Saclay-DESY data [99] at 6 GeV indicate the existence of an appreciable polarization ($P_0 \sim 0.6$) in the process $\pi^-p \to \pi^0n$ at $-t = -0.5$ GeV^2. At the same time, according to the ANL data [100], the polarization in this region is no greater than 0.2 at 5 GeV. However, the results of the amplitude analysis quoted below are insensitive to the value of P_0.

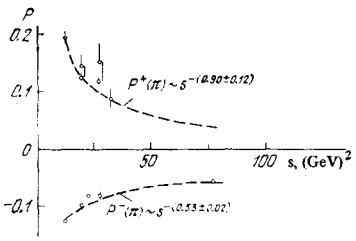

FIG. 21. The energy dependence of the polarization in π^+p scattering ($0.1 \leqslant -t \leqslant 0.3$ $(GeV/c)^2$) [97].

cesses of π^+p and π^-p elastic scattering and the reaction $\pi^-p \to \pi^0 n$, respectively; as a result, it has been possible to carry out a model-independent amplitude analysis of πN scattering[98] (i.e., to determine the phases and moduli of all the πN scattering amplitudes at various values of t). Since the overall phase of the amplitudes is not determined, all the results (Fig. 22) are given in relation to the amplitude f^0_{++}, whose phase is evidently close to $\pi/2$.

The amplitude analysis of πN scattering enables us to draw the following conclusions about the nature of the πN interaction:

a) The amplitude f^0_{++} gives the largest contribution to the differential cross sections.

b) The helicity-changing amplitude with isospin 0 in the t-channel, f^0_{+-}, is much smaller than f^0_{++} and has a phase close to π relative to f^0_{++} throughout the studied range of t. In this connection, the quantity $P_+ + P_-$ is very small. However, the fact that $f^0_{+-} \neq 0$ indicates that the t-channel helicity is not conserved (at any rate, at energies ~ 6 GeV).

c) The differential cross section for charge exchange is determined mainly by the helicity-changing amplitude f^1_{+-}, which has a zero in its real and imaginary parts at $-t = 0.7$ GeV^2, in accordance with the Regge-pole model, in which $f^1_{+-} \sim \alpha_\rho(t)$.

d) The imaginary part of f^1_{++} passes through zero in the region of t which exhibits the cross-over phenomenon of the differential cross sections for $\pi^\pm p$ scattering. The real part of f^1_{++} vanishes at much larger values of $|t|$. The fact that the polarization parameters P(t) and R(t) for the processes of πN scattering do not change in form but merely fall off as a power of the energy offers hope that the main results of the amplitude analysis of πN scattering at 6 GeV will remain valid at higher energies. However, only complete information about the polarization parameters at high energies can provide a definitive answer to this question.

Figure 23 shows new data on the polarization in the processes of elastic K^-p, $\bar{p}p$ and pp scattering.[101] We note that the polarization in $K^\pm p$ and $\bar{p}p$ scattering is close to zero in the region of small momentum transfers $|t| \leqslant 0.3$ GeV^2, in accordance with the predictions of dual models and exchange degeneracy. The energy dependence of the polarization in these processes is shown in Fig. 24.

3.5. Large-angle Scattering

a) **Scattering near $\theta = 90°$ and the problem of the structure of the nucleon.** The experimental data show that the differential cross sections for elastic scattering in the region of large scattering angles and large momentum transfers ($-t \approx u \approx s$) have a strong energy dependence (Fig. 25). The data at large s for fixed scat-

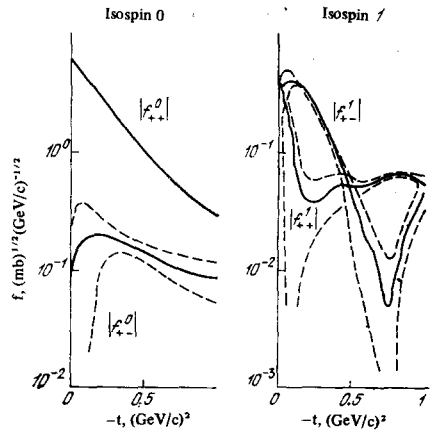

FIG. 22. The results of the amplitude analysis of πN scattering at 6 GeV/c [98].

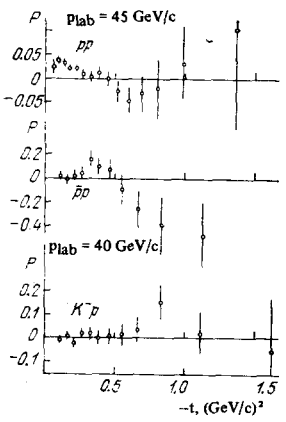

FIG. 23

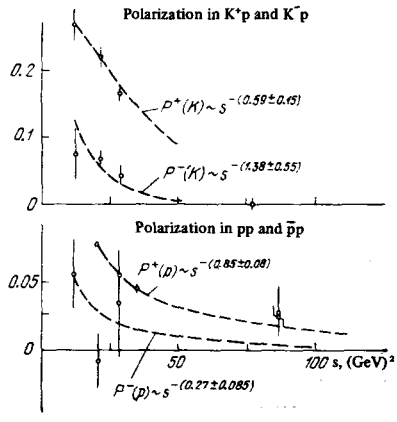

FIG. 24

FIG. 23. Data on the polarization in pp, $\bar{p}p$ and K^-p scattering obtained by the Soviet-French group at Serpukhov [101].

FIG. 24. Energy dependence of the polarization in $K^\pm p$, pp and $\bar{p}p$ scattering [96] ($0.1 \leqslant -t \leqslant 0.3$ $(GeV/c)^2$).

tering angles are described by the power-law dependence $d\sigma/dt \sim s^{-m}$ which was obtained in [102] in the framework of the quark model. A test of this rule is demonstrated in Figs. 25c and 25d, from which it can be seen that the experimental values of the exponents are close to the expected values: m = 10 for pp scattering, and m = 8 for π^-p scattering.

These experiments, like the results of experiments on deep inelastic interactions of leptons, indicate the possible existence of an internal structure of nucleons. The realization that large-angle scattering may be associated with the interaction of point-like particles which make up the structure of hadrons opens new prospects for elementary particle physics.

b) **Backward scattering.** The experimental situation for $\pi^\pm p \to p\pi^\pm$ backward scattering is shown in Fig. 26. The differential cross sections for elastic scattering processes are characterized by the presence of a maximum for backward scattering, where the value of $u = (p_a - p'_b)^2 = \Sigma_i m_i - s - t$ is small. The value of the cross section at the maximum falls off rapidly with energy. In contrast with the maximum for forward scattering (where the variable $-t$ is small and the reaction amplitude is determined by the t-channel singularities, i.e., by the intermediate states in the reaction $a + \bar{a}' \to \bar{b} + b'$, which have boson quantum numbers), backward

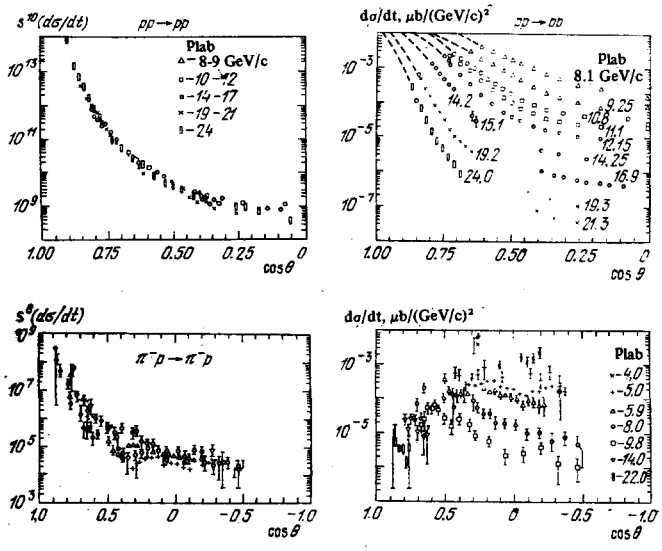

FIG. 25. Comparison of the large-angle cross sections [90] with the predictions of the quark model (the Mateev-Muradyan-Tavkhelidze rule [102]).

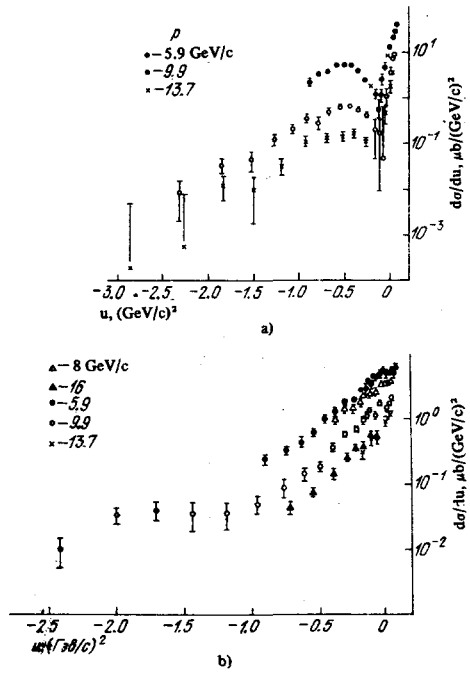

FIG. 26. The differential cross section for a) π^+p and b) π^-p backward scattering in the momentum range from 5.9 to 13.7 GeV/c [104,109].

scattering at small $|u| \sim m^2$ is determined by the u-channel singularities, i.e., by the reaction $a + \bar{b}' \to a' + \bar{b}$. In the processes of elastic $\pi^\pm p$ and K^+p scattering, the quantum numbers of the u-channel singularities correspond to known particles and resonances (such as N and Δ in πN scattering, and Λ, Σ and Y^* in K^+p scattering). At the same time, the u-channels for the K^-p and $\bar{p}p$ reactions correspond to "exotic" quantum numbers; the charge of the system must be equal to -2 in both cases and, in addition, the hypercharge is $Y = -2$ for the $K^-\bar{p}$ system, while the baryon number is $|B| = 2$ for the $\bar{p}\bar{p}$ system. The experimental data (Fig. 27) show [38,103,104] that there is a significant difference between the values of $(d\sigma/dt)_{u=0}$ for the $\pi^\pm p$ and K^+p processes and the "exotic" channels of the backward K^-p and $\bar{p}p$ reactions, even at relatively low energies ($\sim$5 GeV). Moreover,

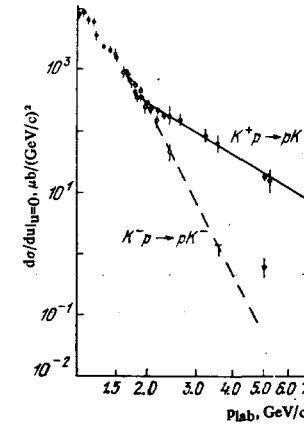

FIG. 27. Energy dependence of $K^\pm p$ scattering at $u \approx 0$ [38].

$(d\sigma/du)_{u=0}$ for K^-p and $\bar{p}p$ scattering falls off with energy much faster ($\sim 1/s^{10}$) than for K^+p or πN scattering. (The data on $K^\pm p$ scattering at u = 0 shown in Fig. 27 are taken from [38].)

Let us consider backward scattering in the framework of the Regge-pole model. As in the case of forward scattering, the differential cross section for a backward scattering process is described by the contribution of the Regge pole which lies furthest to the right in the j-plane (Eq. (2.19) with the substitution $t \to u$). A specific feature of πN and KN backward scattering is that the trajectories have fermion quantum numbers (these trajectories contain particles and resonances with half-integral spins). In this connection, the contribution to the scattering amplitude in the physical region comes from a pair of Regge poles with opposite parity, which are related by the equation [105]

$$\alpha_+(\sqrt{u}) = \alpha_-(-\sqrt{u}). \qquad (3.16)$$

Unlike boson Regge poles, fermion poles depend in general not on the variable u, but on $\sqrt{u}$. By virtue of Eq. (3.16), α_+ and α_- are complex conjugates of one another in the physical scattering region, where $u < 0$: $\alpha_+(\sqrt{u}) = \alpha_-^*\sqrt{u}$.

By analyzing the energy dependence of the differential cross sections for backward scattering, it is possible to determine the trajectories of the Regge poles which give the main contribution to these processes. It is usually assumed that the largest contribution to πN backward scattering processes comes from the N and Δ trajectories. The N trajectory has isospin I = 1/2 and contains the nucleon, i.e., $\alpha_N(m_N^2) = 1/2$; the Δ trajectory has I = 3/2 and passes through the Δ_{1236} isobar. A knowledge of $\alpha_N(0)$ is very important for deciding whether the virtual nucleon is "elementary." If the virtual nucleon which is exchanged in backward scattering is not reggeized and, as an elementary particle, has spin J = 1/2, then, according to Eq. (2.19) with $\alpha_N \equiv 1/2$, the differential cross section must fall off like $\sim 1/s$ for all values of u. A faster decrease of the cross section with energy and a shrinkage of the peak in the angular distribution would indicate that the nucleon, like other particles and resonances, lies on a Regge trajectory. The currently available experimental data on πN backward scattering indicate that the nucleon is reggeized, although this problem must still be regarded as open. An analysis of data [106] on π^-p backward scattering in the range 5–18 GeV implies $\alpha_{eff}(0) = -0.38$ (corresponding to a linear extrapolation of the nucleon trajectory $\alpha_N(u) = \alpha_N(0) + \alpha'_N u$ with a slope $\alpha'_N(0) \approx 1$ GeV^{-2} determined

from the analysis of the spectrum of particles and resonances). However, according to data obtained at Serpukhov,[107] the rate of all-off of $d\sigma/du$ with energy is slower in the region of higher energies, and $\alpha_{eff}(0) \approx 0$. Further studies of backward scattering and backward $\pi^- p$ charge exchange will make it possible to determine $\alpha_{eff}(0)$ more accurately and to obtain additional important information about the properties of baryon exchanges.

Reactions such as $K^- p$ or $\bar{p}p$ backward scattering, which have exotic u-channel quantum numbers, cannot be governed by the exchange of any known Regge poles and are usually described in the framework of complex angular momentum theory by the contributions of moving branch points, i.e., exchanges of several Regge poles in the u-channel. For example, backward $K^- p$ scattering may be determined by the contribution of the $K^* N$ branch point, and $\bar{p}p$ scattering by the NN and ΔN exchanges. Since the position of the appropriate branch point is $\alpha_{12} = \alpha_1 + \alpha_2 - 1$, we have $\alpha_{K^*N}(0) \approx \alpha_{K^*}(0) + \alpha_N(0) - 1 \approx -1$ for $K^- p$ scattering, and $\alpha_{NN}(0) = 2\alpha_N(0) - 1 \approx -1.7$ for pp scattering, i.e., the cross sections for these processes must fall off very rapidly with energy. The simplest estimates based on the graphs of Fig. 4 give very small values for the cross sections of these processes, even at energies ~ 5 GeV. At energies up to ≈ 5 GeV, the cross sections for $K^- p$ and $\bar{p}p$ backward scattering fall off like $\sim s^{-10}$. Complex angular momentum theory predicts that the rate of fall-off of these cross sections with energy is reduced at higher energies to s^{-4} for $K^- p$ scattering and $s^{-5.4}$ for $\bar{p}p$ scattering. It would be of great interest to test this prediction of the theory.

4. CONCLUSIONS

The systematic investigation of elastic scattering processes involving hadrons began 10 years ago, with the development of experimental methods using large accelerators. The results of these investigations, which we have described in the present review, are briefly as follows. Instead of the purely diffractive picture of scattering at high energies ($E > 1$ GeV) which was expected in the 1960s, with a fixed radius of interaction, an imaginary forward scattering amplitude and constant total cross sections, it has been found that there is an appreciable contribution from the real part of the amplitude, which amounts to tens of percent of the imaginary part at 10 GeV. Experiments on pp scattering at Serpukhov and Batavia and colliding-beam experiments at CERN have shown that the ratio of the real part of the amplitude to its imaginary part is negative in absolute value and has a minimum at $E \sim 5$ GeV; it begins to rise as the energy increases, changing sign at $E \approx 280$ GeV.

The total cross sections (and accordingly the imaginary parts of the elastic forward scattering amplitudes) have not reached their constant asymptotic limits; moreover, as was first shown for the Kp interaction at Serpukhov and later in experiments using the CERN storage rings and the extracted beams of the Batavia accelerator, their energy dependence has become qualitatively different: the regime in which the cross sections decrease like $\sigma_t(s) = \sigma_\infty + (a/p^m)$ at energies ≤ 30 GeV has been replaced by a regime of logarithmic growth at energies above 100 GeV.

The slope of the diffraction peak for all elastic scattering processes (except $\bar{N}N$) rises systematically (approximately logarithmically) up to energies $\sim 10^3$ GeV. The rate at which the slope of the peak is rising in pp scattering at energies above 100 GeV is much less than what is observed at energies ~ 10 GeV and corresponds to a relatively small effective value of the slope of the trajectory of the Pomeranchuk pole, $\alpha'_P(0) \approx 0.3$ GeV^{-2}. The experimental data on other elastic processes are consistent with this value of $\alpha'_P(0)$. The non-zero value of α'_P implies that the radius of interaction is increasing with energy.

Measurements within the wide range of energies $3 < E < 200$ GeV have shown that the differences between the total cross sections for the interaction of particles and antiparticles with nucleons are decreasing according to a power law in the studied energy range, in agreement with the Pomeranchuk theorem. The cross sections for charge-exchange reactions such as $\pi^- p \to \pi^0 n$, $K^- p \to K^0 n$ and $\bar{K}^0_L p \to K^0_S p$ are also decreasing according to a power law. These data and the results of measurements of polarization effects are in agreement with the predictions of a theory involving the exchange of reggeized particles: processes governed by exchanges of nonvacuum quantum numbers die out with increasing energy in accordance with the characteristic power law (2.20).

The results of studies of hadronic scattering in the region of large angles and large transverse momenta $p_\perp$, where the contributions due to the t- and u-channel singularities are suppressed, indicate that the scattering in this region is determined by a different mechanism, whose essential feature is the interaction of pointlike particles (quarks or partons) which make up the structure of the nucleon. It appears that this mechanism also shows up in processes involving the production of particles with large transverse momenta.[109] The cross section for the inclusive production of particles with large $p_\perp$ rises rapidly with increasing energy. It would be interesting to determine how this effect influences the behavior of the total cross sections for hadronic interactions.[110] The growth of σ_t might have a threshold character. In this case, the region of energies $s \sim 10^2$ GeV^2 would be not the beginning of the asymptotic region, but a threshold at which new physical phenomena begin.

We note that the trends which are observed in the existing experimental data indicate that the region of energies $s \sim 10^3$ GeV^2 is not yet the asymptotic region. In fact, if the total cross section $\sigma_t(s)$ and the slope of the peak $B(s)$ continued to have dependences of the form (3.2) and (3.9) as $s \to \infty$, there would be a violation of the unitarity condition, according to which[111] $B(s) \geq \sigma_t/18\pi$; i.e., the slope cannot grow asymptotically more slowly than the total cross section, as is implied by the empirical dependences (3.2) and (3.9).

Thus, the study of elastic scattering processes at high energies has significantly extended and deepened our conceptions of the characteristic properties of the strong interactions. It has led to the emergence of a number of new interesting ideas and approaches to the problem of hadronic interactions at high energies. However, in spite of the significant extension of the range of studied energies, we are still not able to provide definitive answers to some important questions: Does the total cross section tend to a constant limit, or does it continue to grow indefinitely as $s \to \infty$? If the growth continues, what law does it follow? Does the logarithmic shrinkage of the

peak continue at higher energies? Does the real part of the amplitude tend to zero as $s \to \infty$?

A solution of these problems calls for new high-precision experiments at existing energies and the study of scattering processes at higher energies.

[1]N. N. Bogolyubov, B. V. Medvedev, and M. K. Polivanov, Voprosy teorii dispersionnykh sootnosheniĭ (Problems of the Theory of Dispersion Relations), Moscow, Fizmatgiz, 1958.
[2]M. Froissart, Phys. Rev. **123**, 1053 (1961).
[3]M. L. Goldberger, Relations de Despersion et Particules Elementies (Les Houches), Paris, Hermann, 1960.
[4]G. Höhler, G. Ebel, and J. Giesecke, Zs. Phys. 180, 430 (1964). G. Höhler and R. Strauss, Tables of Pion-Nucleon Forward Amplitudes, Preprint, University of Karlsruhe, 1970.
[5]I. Ya. Pomeranchuk, Zh. Eksp. Teor. Fiz. **34**, 725 (1958) [Sov. Phys.-JETP **7**, 499 (1958)].
[6]N. N. Meĭman, Zh. Eksp. Teor. Fiz. **43**, 2277 (1962) [Sov. Phys.-JETP **16**, 1609 (1963)].
[7]A. A. Logunov, Nguen Van Hieu and I. T. Todorov, Usp. Fiz. Nauk **88**, 51 (1966) [Sov. Phys.-Usp. **9**, 31 (1966)]. A. A. Logunov, M. A. Mestvirishvili and O. A. Khrustalev, Probl. fiz. ÉChAYa **3**, 515 (1972) [Sov. J. Part. Nuclei **3**, 261 (1972)].
[8]Yu. S. Vernov, Teor. Mat. Fiz. **4**, 3 (1970).
[9]A. Martin, Scattering Theory, Unitarity, Analyticity and Crossing, Lecture Notes in Physics, No. 3, Berlin, Springer-Verlag, 1969. F. J. Yndurain, Rev. Mod. Phys. **44**, 645 (1972). S. M. Roy, Phys. Rept. **5C**, 125 (1972).
[10]V. G. Grishin, I. S. Saitov, and I. V. Chuvilo, Zh. Eksp. Teor. Fiz. **34**, 1221 (1958) [Sov. Phys.-JETP **7**, 844 (1958)]. D. I. Blokhintsev, V. S. Barashenkov, and V. G. Grishin, ibid. **35**, 311 (1959) [**8**, 215 (1959)].
[11]K. A. Ter-Martirosyan, in: Voprosy fiziki élementarnykh chastits (Problems of Elementary Particle Physics), No. 5, Erevan, Armenian Academy of Sciences, 1966, p. 479.
[12]E. Leader, Rev. Mod. Phys. **38**, 467 (1966).
[13]P. D. B. Collins and E. J. Squires, Regge Poles in Particle Physics, Berlin, Springer-Verlag, 1968 [Russ. Transl., Moscow, Mir, 1971].
[14]V. N. Gribov, I. Ya. Pomeranchuk, and K. A. Ter-Martirosyan, Yad. Fiz. **2**, 361 (1965) [Sov. J. Nucl. Phys. **2**, 258 (1966)].
[15]A. B. Kaĭdalov, in: Élementarnye chastitsy (Elementary Particles), No. 2, Moscow, Atomizdat, 1973, p. 18.
[16]K. A. Ter-Martirosyan, Yad. Fiz. **10**, 1047 (1969) [Sov. J. Nucl. Phys. **10**, 600 (1970)].
[17]K. G. Boreskov, A. M. Lapidus et al., Yad. Fiz. **14**, 814 (1971) [Sov. J. Nucl. Phys. **14**, 457 (1972)].
[18]Chan Hong-Mo, in: Proc. of the 14th Intern. Conf. on High Energy Physics, Geneva, 1968, p. 391. R. J. Glauber, in: Lectures in Theoretical Physics, Vol. 1, New York, Interscience, 1959, p. 1.
[19]a) V. N. Gribov and A. A. Migdal, in: 14th Intern. Conf. on High Energy Physics, Vienna, 1968, papers 943, 944. b) V. Yu. Glebov et al., Yad. Fiz. **10**, 1065 (1969) [Sov. J. Nucl. Phys. **10**, 609 (1970)]. c) F. Frautschi and B. Margolis, cited in [19a], paper 727. d) A. I. Lendel and K. A. Ter-Martirosyan, ZhETF Pis. Red. **11**, 70 (1970) [JETP Lett. **11**, 45 (1970)].
[20]A. A. Logunov and A. N. Tavkhelidze, Nuovo Cimento **29**, 380 (1963).
[21]V. R. Garsevanishvili et al., Phys. Lett. **B29**, 191 (1969).
[22]A. Tavkelidze, in: High Energy Physics, Kiev, Naukova Dumka, 1972, p. 367.
[23]A. A. Ansel'm and I. T. Dyatlov, Yad. Fiz. **6**, 591, 603 (1967) [Sov. J. Nucl. Phys. **6**, 430, 439 (1968)]; **9**, 416 (1969) [**9**, 242 (1969)].
[24]E. M. Levin and L. L. Frankfurt, ZhETF Pis. Red. **2**, 105 (1965) [JETP Lett. **2**, 65 (1965)]; Usp. Fiz. Nauk **94**, 244 (1968) [Sov. Phys.-Usp. **11**, 106 (1968)]. R. Muradyan, JINR Preprint R2-6762, Dubna, 1972.
[25]V. Matveev, R. Muradyan, and A. Tavkhelidze, Nuovo Cimento Lett. **7**, 719 (1973). S. J. Brodsky and G. R. Farrar, Phys. Rev. Lett. **31**, 1153 (1973).
[26]V. A. Nikitin, V. A. Sviridov et al., Zh. Eksp. Teor. Fiz. **46**, 1608 (1964) [Sov. Phys.-JETP **19**, 1086 (1964)].
[27]B. Bekker et al., in: Proc. of the 11th Conf. on High Energy Physics, Geneva, 1962, p. 582. L. F. Kirillova et al., Zh. Eksp. Teor. Fiz. **45**, 1261 (1963) [Sov. Phys.-JETP **18**, 867 (1964)]; Phys. Lett. **13**, 93 (1964).
[28]G. G. Beznogikh et al., Yad. Fiz. **10**, 1212 (1969) [Sov. J. Nucl. Phys. **10**, 687 (1970)]; Phys. Lett. **B30**, 274 (1969).
[29]G. G. Beznogikh et al., ibid. **B39**, 411 (1972).
[30]V. Bartenev et al., Phys. Rev. Lett. **31**, 1088 (1973).
[31]V. Bartenev et al., ibid., p. 1367.
[32]V. A. Nikitin, A. A. Nomofilov, V. A. Sviridov, L. A. Slepets, I. M. Sitnik, and L. N. Strunov, Yad. Fiz. **1**, 183 (1965) [Sov. J. Nucl. Phys. **1**, 127 (1965)]. L. S. Zolin, A. A. Nomofilov, I. M. Sitnik, L. A. Slepets, and L. N. Strunov, ZhETF Pis. Red. **6**, 546 (1967) [JETP Lett. **6**, 546 (1967) [JETP Lett. **6**, 65 (1967)]; Phys. Lett. **22**, 350 (1966).
[33]K. J. Foley et al., Phys. Rev. **181**, 1775 (1969); Phys. Rev. Lett. **19**, 193, 330 (1967).
[34]A. A. Borisov et al., IHEP Preprint SÉF-72-7, Serpukhov, 1972.
[35]G. Bellettini et al., Phys. Lett. **14**, 164 (1965); **19**, 705 (1966). A. E. Taylor et al., ibid. **14**, 54 (1965).
[36]I. V. Chuvilo et al., in: Proc. of the Intern. Conf. on Instrumentation for High Energy Physics (Stanford University, September 1966), Springfield, 1966, p. 579. G. G. Vorob'ev et al., JINR Preprint R1-4445, 1969; E1-7552, 1973.
[37]M. Borghini et al., Nucl. Instr. and Meth. **105**, 215 (1972).
[38]V. Chabaud et al., Phys. Rev. Lett. **B38**, 441, 445, 449 (1972).
[39]S. P. Denisov et al., Phys. Lett. **B36**, 415, 528 (1971).
[40]U. Amaldi et al., ibid. **B44**, 112 (1973).
[41]S. R. Amendolia et al., ibid., p. 119.
[42]N. L. Grigorov et al., in: Proc. of the 9th Intern. Conf. on Cosmic Rays, London, 1965, p. 860.
[43]A. S. Carroll et al., Phys. Rev. Lett. **33**, 928, 932 (1974).
[44]Yu. P. Gorin et al., Yad. Fiz. **17**, 309 (1973) [Sov. J. Nucl. Phys. **17**, 157 (1973)].
[45]V. K. Birulev et al., Yad. Fiz. **15**, 959 (1972) [Sov. J. Nucl. Phys. **15**, 534 (1972)].
[46]H. Bethe, Ann. Phys. (N.Y.) **3**, 190 (1958). M. P. Locher, Nucl. Phys. **B2**, 525 (1967). C. B. West and D. R. Yennie, Phys. Rev. **172**, 1413 (1968). L. D. Soloviev and A. V. Schelkachev, Nucl. Phys. **B40**, 596 (1972). V. G. Gorshkov et al., Zh. Eksp. Teor. Fiz. **60**, 1211 (1971) [Sov. Phys.-JETP **33**, 655 (1971)]. V. M. Budnev and I. F. Ginzburg, ZhETF Pis. Red. **13**, 519 (1971) [JETP Lett. **13**, 370 (1971)].
[47]P. Söding, Phys. Lett. **8**, 283 (1964).

[48]I. I. Levintov and G. M. Adelson-Velsky, ibid. 13, 185 (1964). V. S. Barashenkov and V. I. Dedu, Nucl. Phys. 64, 636 (1965).
[49]A. A. Vorobyov et al., Phys. Lett. B41, 639 (1972).
[50]G. Höhler and H. P. Jakob, Zs. Phys. 268, 75 (1974); Karlsruhe Preprint TKP 9/74, 1974.
[51]L. F. Kirillova et al., Yad. Fiz. 1, 533 (1965) [Sov. J. Nucl. Phys. 1, 379 (1965)].
[52]N. Dalkhazhavi et al., Yad. Fiz. 8, 342 (1968) [Sov. J. Nucl. Phys. 8, 196 (1969)].
[53]U. Amaldi et al., Phys. Lett. B43, 231 (1973).
[54]R. C. Fernow et al., ibid. B52, 243 (1974).
[55]C. Bourrely, J. Soffer, and D. Wray, Nucl. Phys. B77, 386 (1974).
[56]T. Khuri and T. Kinoshita, Phys. Rev. B137, 720; B140, 706 (1965).
[57]Yu. S. Vernov, Zh. Eksp. Teor. Fiz. 53, 191 (1967) [Sov. Phys.-JETP 26, 130 (1968)].
[58]G. G. Volkov, IHEP Preprint STF-71-8, Serpukhov, 1971.
[59]U. P. Sukhatme and J. N. Ng, Nucl. Phys. B70, 229 (1974).
[60]E. Leader and U. Maor, Phys. Lett. B43, 505 (1973).
[61]W. von Schlippe and D. W. Joynson, Preprint, Westfield College, London, May 1974.
[62]T. H. Bellm et al., Nuovo Cimento Lett. 3, 389 (1970); Phys. Lett. B33, 438 (1970).
[63]R. Campbelle et al., Nucl. Phys. B64, 1 (1973).
[64]P. Baillon et al., Phys. Lett. B50, 377, 383 (1974).
[65]C. W. Brandenburg et al., Preprint SLAC-PUB-1339, 1973.
[66]A. D. Brody et al., Phys. Rev. Lett. 26, 1050 (1971). P. Darriulat et al., Phys. Lett. B33, 470 (1970).
[67]K. F. Albrecht et al., ibid. B48, 257 (1974). D. Freytag et al., Report submitted to the Aix Conference, 1973.
[68]R. J. N. Phillips, Nucl. Phys. B72, 481 (1974).
[69]G. G. Vorob'ev et al., Yad. Fiz. 19, 849 (1974) [Sov. J. Nucl. Phys. 19, 433 (1974)].
[70]V. D. Apokin et al., in: 17th Intern. Conf. on High Energy Physics, London, 1974, paper 786.
[71]V. D. Apokin et al., ibid., paper 786.
[72]P. Baillon et al., Phys. Lett. B50, 387 (1974).
[73]R. Oehme, Phys. Rev. 100, 1503 (1955).
[74]D. I. Blokhintsev, Usp. Fiz. Nauk 89, 185 (1966).
[75]P. H. Eberhard, CERN/D, Ph. 11/PHYS 72-38. M. Kupczynski, Phys. Lett. B47, 224 (1973); cited in [70], papers 58–62.
[76]G. Höhler and P. Kroll, Phys. Lett. B49, 280 (1974).
[77]U. Amaldi et al., ibid. B36, 504 (1971).
[78]G. Barbillini et al., ibid. B39, 663 (1972).
[79]T. Lasinski et al., Phys. Rev. 179, 1426 (1969); Nucl. Phys. B37, 1 (1972).
[80]C. W. Akerlof et al., Michigan Preprint UM-HE-74-20, 1974; cited in [70], paper 492.
[81]A. A. Derevshchikov et al., Nucl. Phys. B80, 442 (1974).
[82]Yu. M. Antipov et al., ibid. B57, 333 (1973).
[83]A. A. Derevshchikov et al., Phys. Lett. B48, 367 (1974).
[84]Yu. M. Antipov et al., Preprint IHEP 74-99, 1974.
[85]I. Ambats et al., Phys. Rev. D9, 1179 (1974).
[86]R. A. Carrigan, Phys. Rev. Lett. 24, 168 (1970).
[87]D. Birnbaum et al., cited in [70], paper 770.
[88]A. Anselm and V. Gribov, Phys. Lett. B40, 487 (1972).
[89]O. V. Dumbrajs et al., Nucl. Phys. B69, 336 (1974).
[90]V. Barger, Reaction Mechanisms at High Energy, Plenary Session Talk at the 17th Intern. Conf. on High Energy Physics, London, 1974.
[91]R. Henzi and P. Valin, Phys. Lett. B48, 119 (1973).
[92]E. Nagy et al., cited in [70], paper 488.
[93]A. J. Buras and J. Dias de Deus, Nucl. Phys. B71, 481 (1974).
[94]M. Borghini et al., Phys. Lett. B36, 493, 497, 501 (1971).
[95]C. Bruneton et al., ibid. B44, 471 (1973).
[96]A. N. Diddens, Rapporteur's talk at the 17th Intern. Conf. on High Energy Physics, London, 1974.
[97]A. De Lesquen et al., Phys. Lett. B40, 277 (1972).
[98]G. Gozzika et al., ibid., p. 281.
[99]P. Bomamy et al., Nucl. Phys. B52, 382 (1973).
[100]D. H. Hill et al., Phys. Rev. Lett. 30, 239 (1973).
[101]A. Gaidot et al., cited in [70], papers 782, 783, 1019.
[102]V. Matveev, R. Muradyan, and A. Tavkhelidze, Nuovo Cimento Lett. 5, 907 (1972); JINR Preprint D2-7110, Dubna, 1973.
[103]D. P. Owen et al., Phys. Rev. 181, 1794 (1969).
[104]E. W. Anderson et al., Phys. Rev. Lett. 20, 1529 (1968).
[105]V. N. Gribov, Zh. Eksp. Teor. Fiz. 43, 1529 (1962) [Sov. Phys.-JETP 16, 1080 (1963)].
[106]D. P. Owen et al., Phys. Rev. 18, 1794 (1969). W. F. Baker et al., Nucl. Phys. B25, 385 (1971).
[107]A. Babaev et al., Phys. Lett. B38, 342 (1972).
[108]M. Jacob, CERN Preprint 74-15, 31 July 1974.
[109]B. Alper et al., Phys. Lett. B44, 521, 527 (1973). M. Banner et al., ibid., p. 537. F. W. Büsser et al., ibid. B46, 471 (1973).
[110]F. Halzen, Preprint, University of Wisconsin, June 1974.
[111]S. W. MacDowell and A. Martin, Phys. Rev. B135, 960 (1964).

Translated by N. M. Queen